

Addendum for the paper “*The Dynamics of
Exploitation and Class in Accumulation
Economies*”. Not for publication.

Jonathan F. Cogliano,^{*} Roberto Veneziani,[†] and Naoki Yoshihara[‡]

November 30, 2015

Abstract

Section 1 demonstrates that in all of the simulations, conditions (b)-(d) of Definition 1 are satisfied. Sections 2-5 present the results of the robustness checks.

^{*}(Corresponding author) Department of Economics, Dickinson College, Althouse 112, P.O. Box 1773 Carlisle, PA 17013, U.S. (coglianj@dickinson.edu)

[†]School of Economics and Finance, Queen Mary University of London, Mile End Road, London E1 4NS, UK. (r.veneziani@qmul.ac.uk)

[‡]The Institute of Economic Research, Hitotsubashi University, Naka 2-1, Kunitachi, Tokyo 186-0004, Japan. (yosihara@ier.hit-u.ac.jp)

1 Equilibrium conditions

The Figures in this section show that, in all of our simulations, conditions (b)-(d) of Definition 1 in the paper are satisfied, and so we are analysing the equilibrium dynamics of the economies considered.

Figure 1: Equilibrium conditions - Basic model

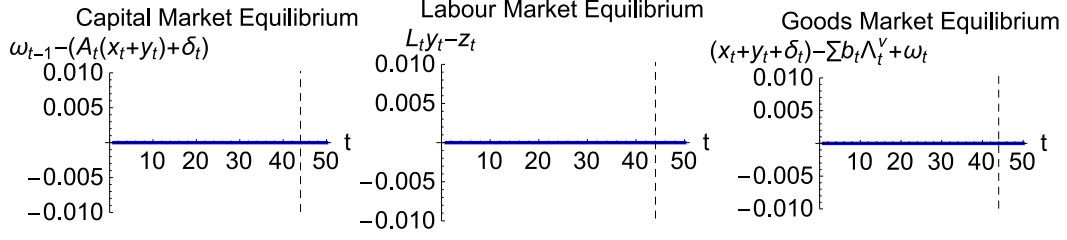


Figure 2: Equilibrium conditions - Model with exogenous technical change and population growth

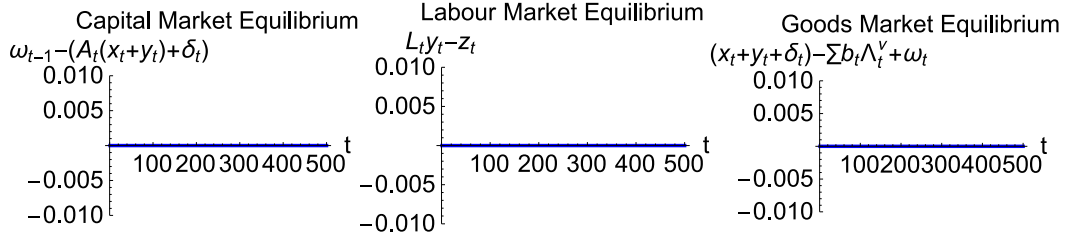


Figure 3: Equilibrium conditions - Bargaining model with $\epsilon = 0$

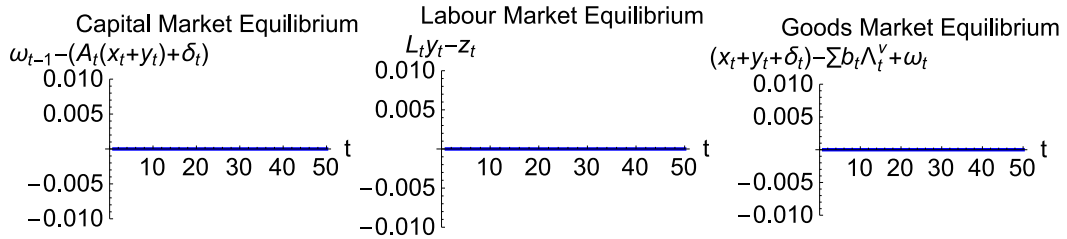


Figure 4: Equilibrium conditions - Bargaining model with $\epsilon = 1$

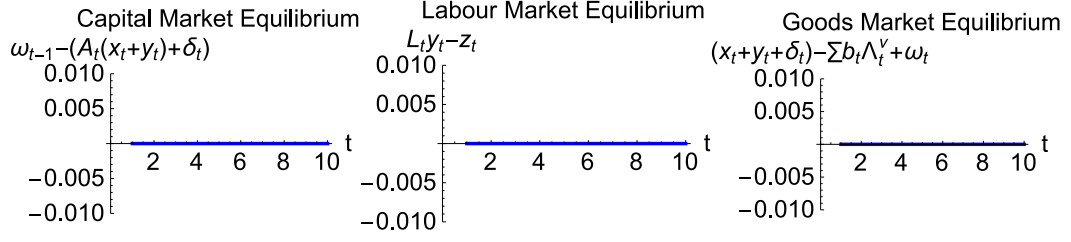
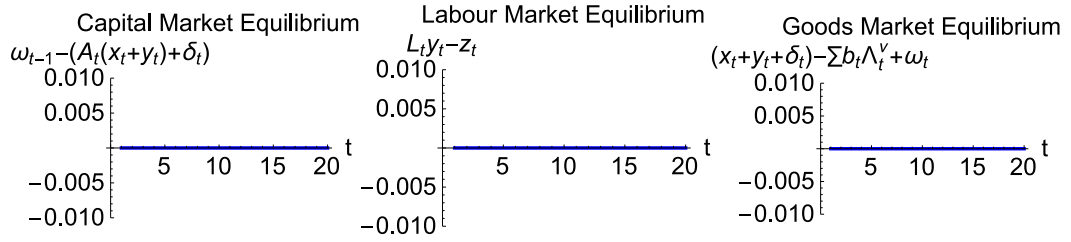


Figure 5: Equilibrium conditions - Bargaining model with $\epsilon = 0.002$



2 An alternative analysis of technical change

In this section, we analyse two variants of the model with exogenous technical change and population growth in section 7 of the paper. The first modifies the basic model of section 6 to include only exogenous technical change. The second includes only population growth.

2.1 Exogenous technical change

This version of the basic model, starting in a capital-constrained state, incorporates an exogenous, constant rate of technological progress and endogenously determined subsistence to explore how technical change alone can maintain capital scarcity. Technological progress is such that A_t remains constant and L_t decreases by two percent during each t . Subsistence b_t grows at the same rate as the aggregate endowment. The number of agents N is constant at 100 and the initial distribution of endowments is handled as in sections 6 and 7 of the paper, as are all other parameters.

The results of the simulation are presented in Figures 6-10(b). Figure 6 presents the summary results, which are qualitatively similar to those in section 7 of the paper. The similarities are clear in terms of g_t and π_t quickly settling to steady rates, and with z_t remaining constant. The simulation remains capital constrained for all t , thus $\hat{w}_t = b_t$ for all t . Figure 7 shows L_t and labour values over the course of the simulation.

Figure 8 shows the exploitation and class status of the agents over the course of the simulation. Both the basic structure of exploitation relations and the class structure are identical to those shown in section 7 of the paper. As in section 7, because the simulation remains capital constrained, exploitation and classes persist, and, because $L_t y_t$ remains constant for all t , the class structure remains stable over the simulation.

Figures 9(a) and 9(c) show the stable distribution of e_t' across agents for all t in Figure 9(a) and more clearly for select t in Figure 9(c). Figure 9(b) shows that the Gini coefficient of e_t' quickly settles to a stable level over the simulation.

Figures 10(a) and 10(b) show the distribution of wealth in terms of the Gini coefficient and for select t . As in section 7, wealth inequalities are persistent and worsen over time. In particular, Figure 10(b) shows the wealth of agents in upper classes growing ever distant from that of agents in the lower classes. The stable Gini coefficient in Figure 10(a) may be counterintuitive but it is a result of mechanisms discussed in section 6 of the paper.

Figure 6: Summary results - Model with exogenous technical change

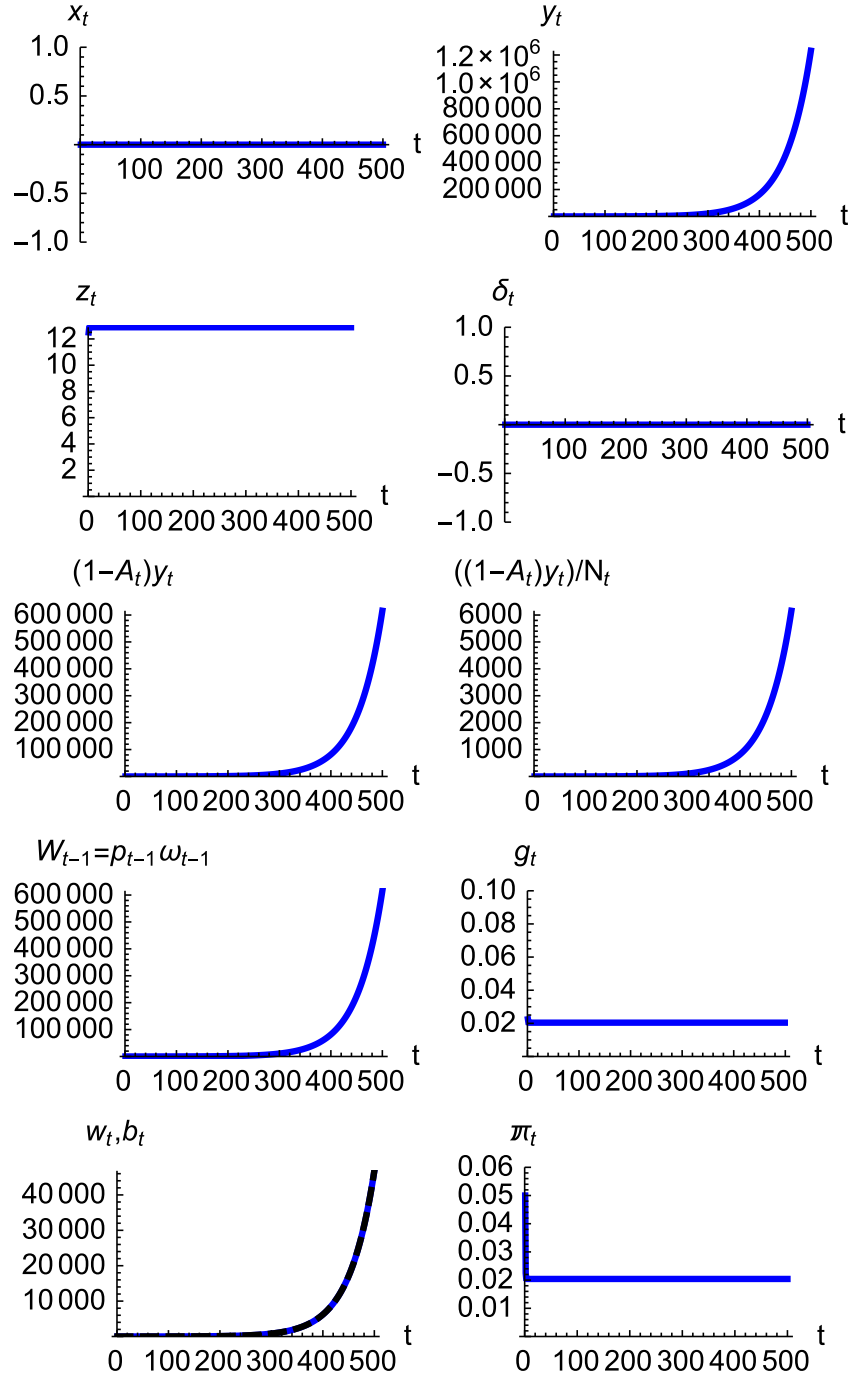


Figure 7: L_t and labour values - Model with exogenous technical change

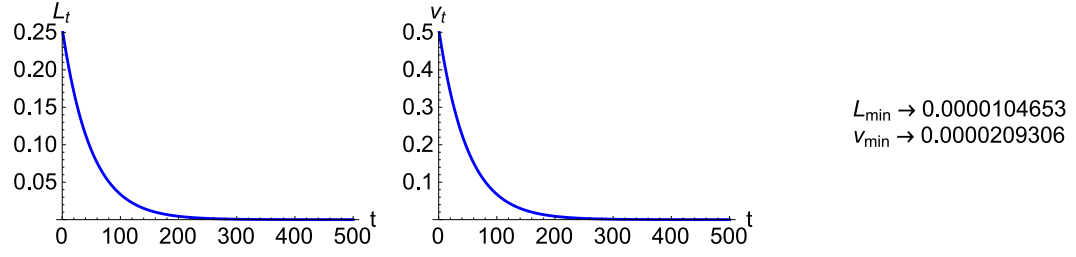


Figure 8: Class and exploitation status - Model with exogenous technical change

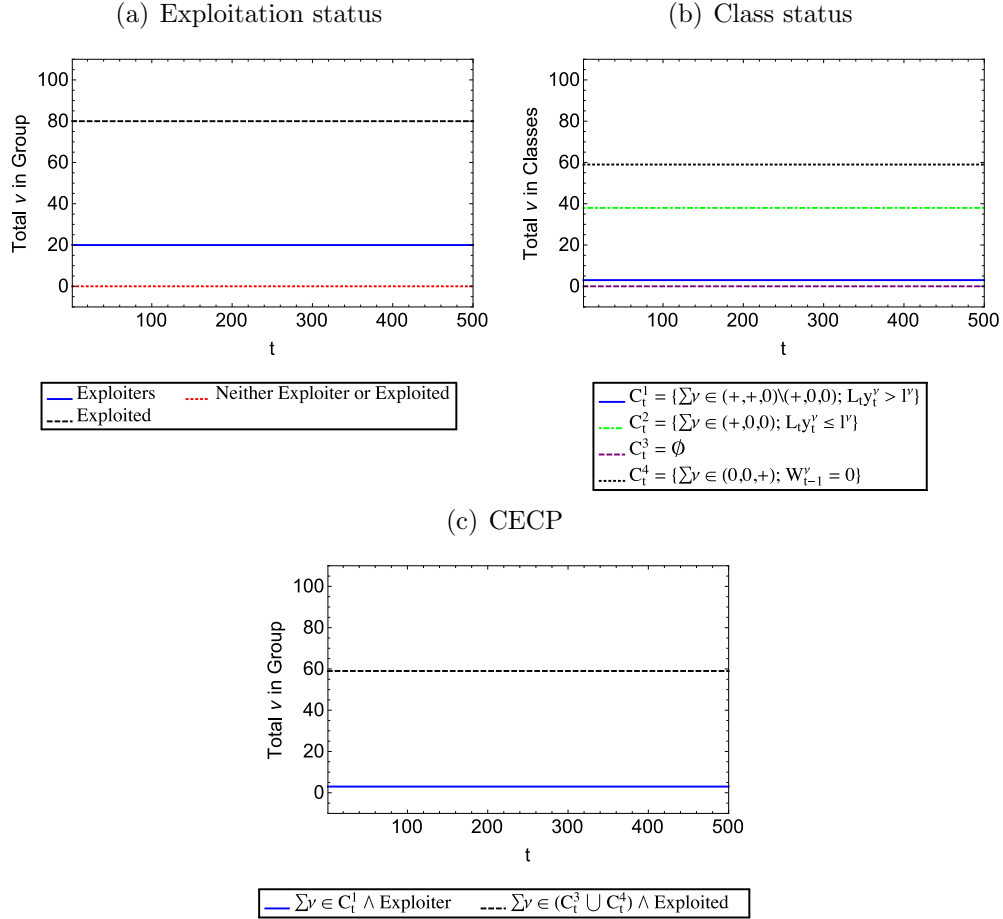
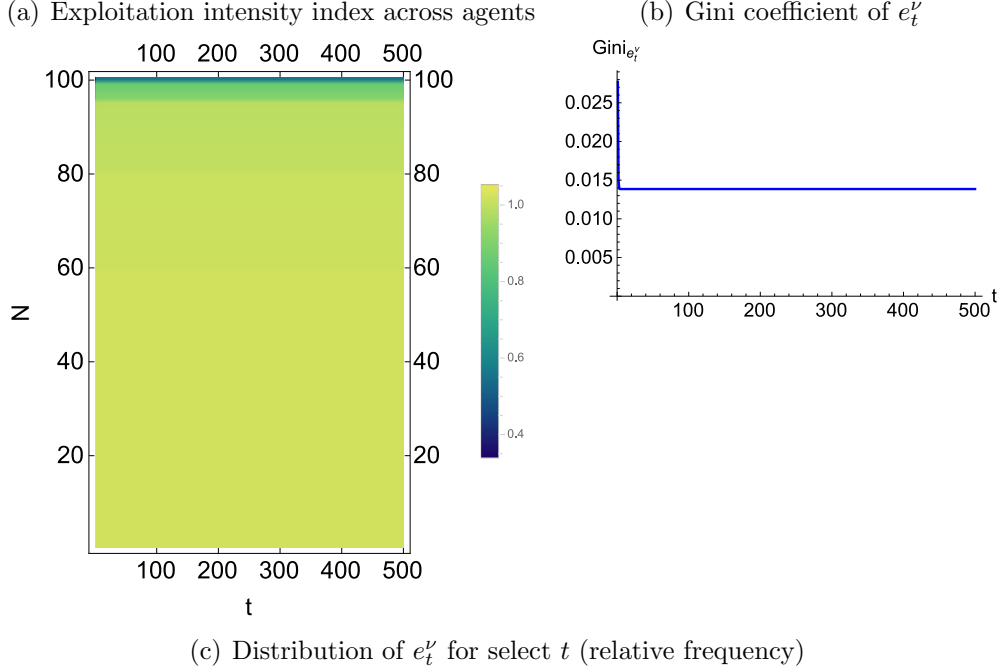


Figure 9: Exploitation intensity index - Model with exogenous technical change

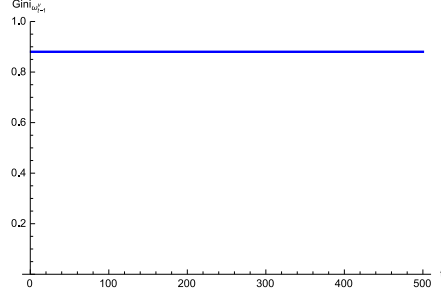


2.2 Population growth

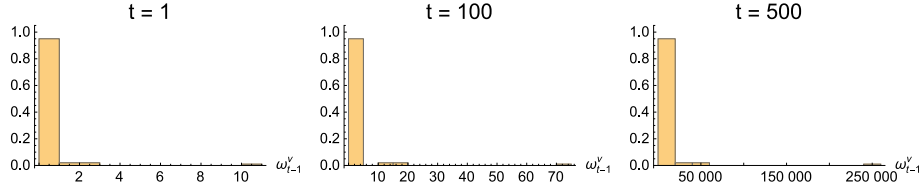
In this section we incorporate exogenous population growth in the basic model to demonstrate that population growth *can* (contribute to) maintain capital scarcity. We set $N_0 = 100$ and the initial distribution of endowments is determined as in the other simulations. During each t the population grows at a rate of roughly five percent. The growth rate is approximate since the size of the population must be rounded to the nearest integer. New agents enter the simulation with $\omega_{t-1}^\nu = 0$. Technology (A, L) and the consumption

Figure 10: Distribution of wealth - Model with exogenous technical change

(a) Gini coefficient of wealth



(b) Distribution of wealth for select t (relative frequency)



standard b are constant. All other parameters are the same as in sections 6 and 7 of the paper.

The results reported below are for a case in which the (roughly constant) rate of population growth, \hat{N} , is large enough to maintain the capital-constrained state for all t . For population growth to maintain capital scarcity $\hat{N} \geq g_t$ for all t .¹ Below, we shall report the results for the case with $g_t = \hat{N}$ for the sake of expositional convenience. The results are qualitatively the same if one considers the case with $g_t < \hat{N}$.

The results of the simulation are reported in Figures 11-14(b). Figure 11 displays the summary results, which show that g_t and π_t remain constant while z_t increases with population growth. Because \hat{N} is high enough to maintain capital scarcity, $\hat{w}_t = b_t = b$ for all t . The figure showing A_t , L_t , and v_t is omitted because all technological variables remain constant.

¹If $\hat{N} < g_t$ then, as endowments grow, z_t^ν grows for all ν and the economy eventually becomes labour constrained (albeit possibly only after a very long time). In this case, the results are qualitatively similar to those reported in section 6 of the paper.

Figure 11: Summary results - Model with population growth

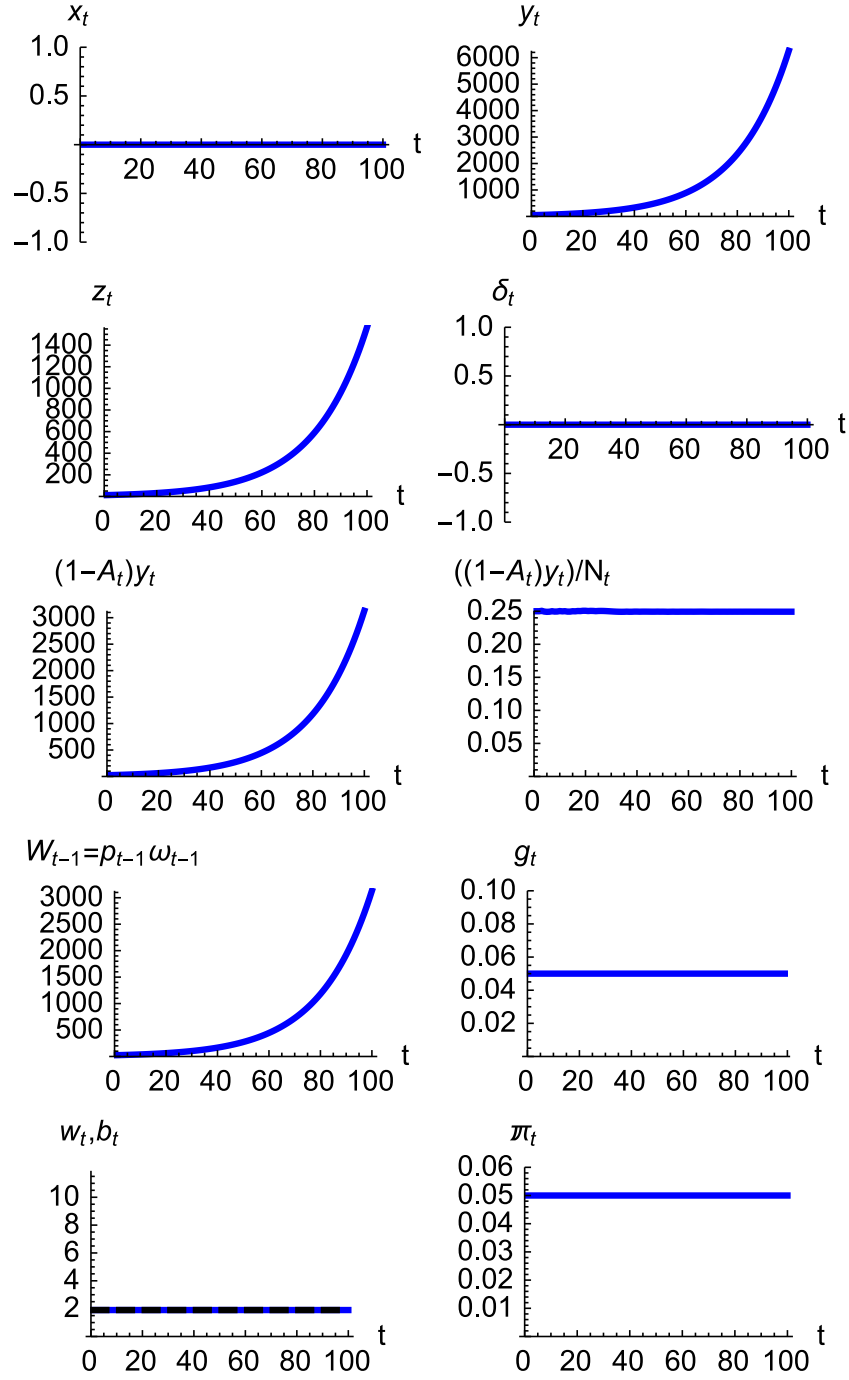


Figure 12: Class and exploitation status - Model with population growth

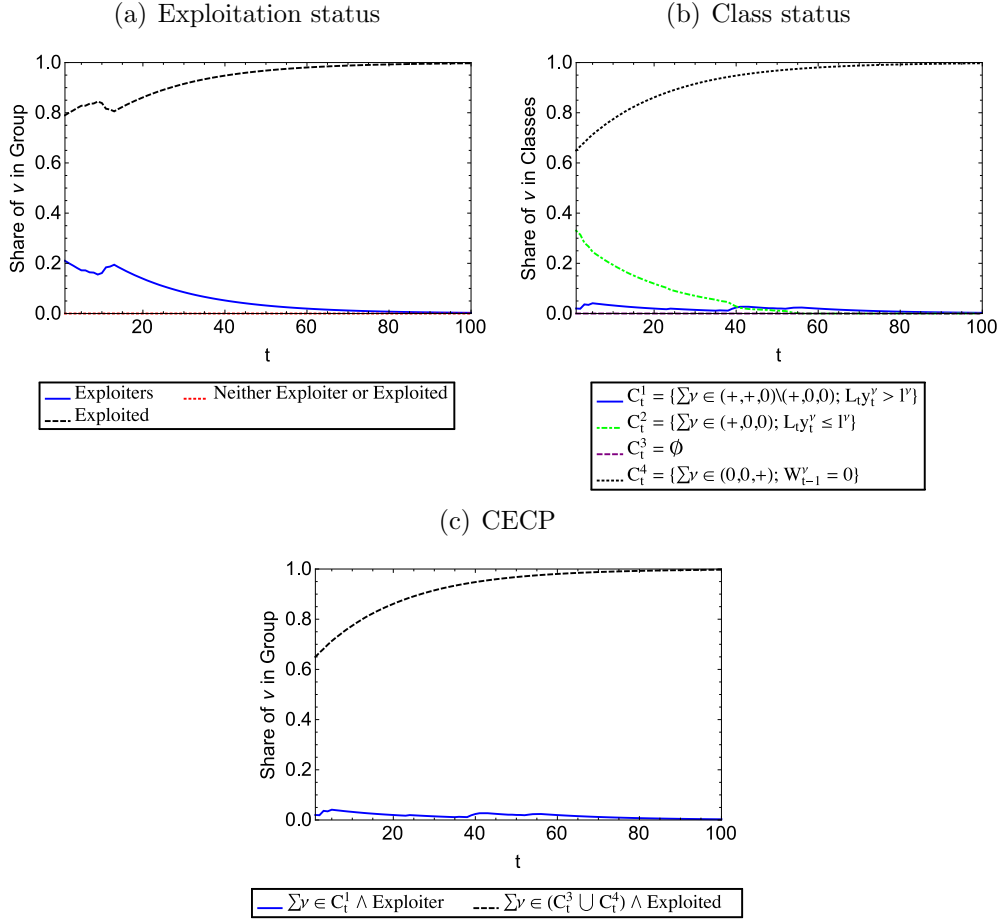


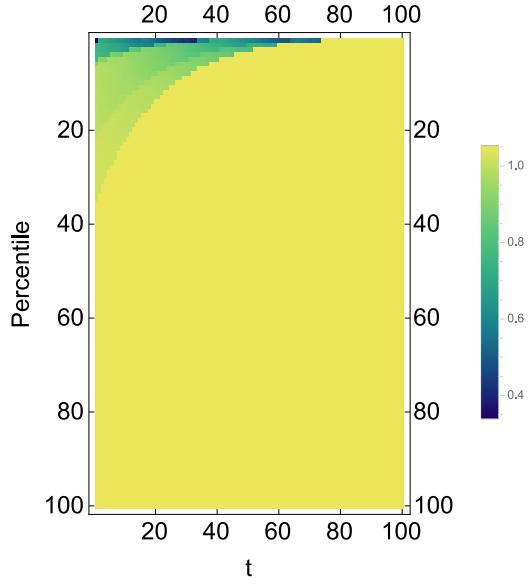
Figure 12 shows the exploitation and class status of agents. All figures show the same type of polarisation of the economy as in section 7. As propertyless agents join the economy, the ranks of the exploited and the number of agents in C_t^4 increase as a percentage of the overall population.

Figures 13(a)-13(c) show the distribution of e_t^v by percentile, the Gini coefficient of e_t^v , and the distribution of e_t^v for select t . All figures reinforce the polarisation of exploitation depicted in Figure 12(a). The Gini coefficient of e_t^v in Figure 13(b) is decreasing for the same reasons discussed in section 7 of the paper.

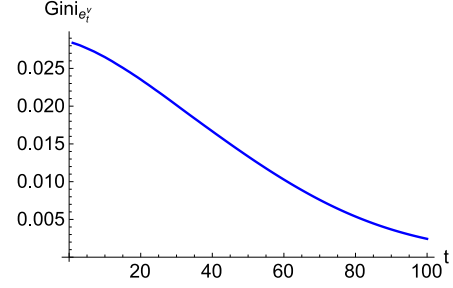
Figures 14(a) and 14(b) depict the Gini coefficient of wealth and the distribution of ω_{t-1} for select t . These figures also show a polarisation of wealth over time as a greater share of the population never accumulates.

Figure 13: Exploitation intensity index - Model with population growth

(a) Exploitation intensity index across agents



(b) Gini coefficient of e_t^ν



(c) Distribution of e_t^ν for select t (relative frequency)

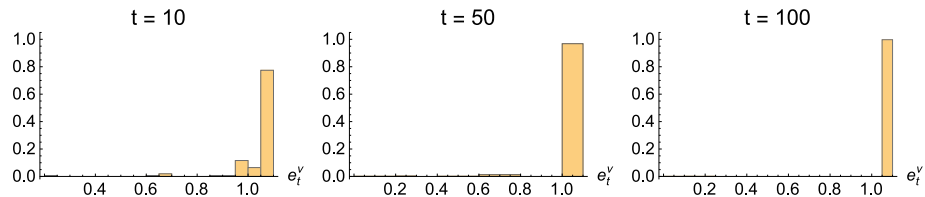
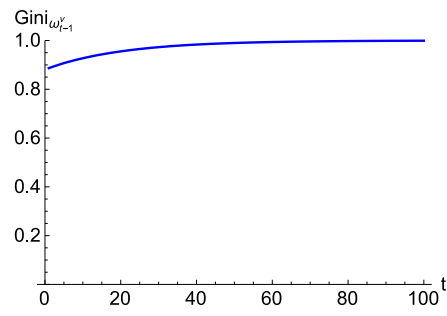
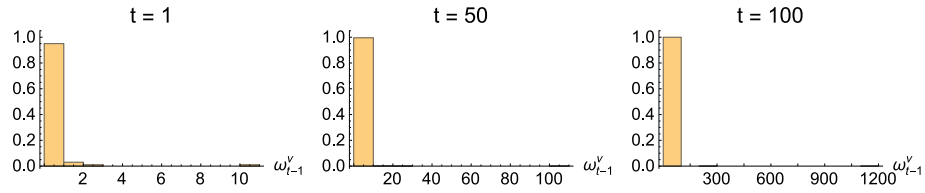


Figure 14: Distribution of wealth - Model with population growth

(a) Gini coefficient of wealth



(b) Distribution of wealth for select t (relative frequency)



3 Alternative to the bargaining model

This section introduces a variation of the bargaining model in section 8 of the paper. In this version the bargaining mechanism and population dynamics are as in section 8, but we introduce exogenous labour-saving technical change whereby A_t remains constant and L_t decreases by two percent during each t . All initial values and parameters are the same as in section 8, and we explore the behaviour of the model with different values of ϵ . The simulation occurs in the following order: (1) determine the bargaining power distribution; (2) determine \hat{w}_t and π_t ; (3) agents solve MP_t^ν ; (4) L_{t+1} is adjusted downward; (5) population growth occurs to balance the knife-edge condition; and (6) steps (2)-(5) are repeated for T .

3.1 Bargaining model with exogenous technical change and population growth, $\epsilon = 0$

This section examines the bargaining model with exogenous technical change and $\epsilon = 0$. Figure 15 reports the summary results, which show that the economy grows smoothly as π_t and g_t steadily rise while $\hat{w}_t = b_t$ for all t due to the lack of bargaining power for those agents with $\omega_{t-1}^\nu = 0$. Figure 16 reports L_t and labour values for t .

Figure 17 reports the exploitation and class status of agents. It is evident from the panels below that the economy becomes increasingly polarised in terms of exploitation and class status. As the population grows and new agents arrive with $\omega_{t-1}^\nu = 0$ they join C_t^4 and remain there for all t . Similarly, agents who begin in C_t^1 remain there, but are eventually joined by agents who begin in C_t^2 and eventually experience $L_t y_t^\nu > l^\nu$ with C_t^2 being empty by the end of the simulation.

Figure 18 describes the distribution of the exploitation intensity index. Figure 18(a) shows the distribution of e_t^ν by percentile over the course of the simulation, which confirms the polarisation observable in Figure 17: by the end of the simulation the vast majority of the population is experiencing increasing exploitation intensity - a pattern clearly visible also in Figure 18(c), which shows the distribution of e_t^ν for select t . Figure 18(b) shows the Gini coefficient of e_t^ν , which decreases over time due to an increasing number of agents with $\omega_{t-1}^\nu = 0$ experiencing $e_t^\nu > 1$ (see section 7 of the paper).

Figures 19(a) and 19(b) show the Gini coefficient of wealth and the distribution of wealth for select t . As expected, the Gini coefficient of wealth increases over t and asymptotically approaches one, reflecting a polarisation

Figure 15: Summary results - Bargaining model with exogenous technical change with $\epsilon = 0$

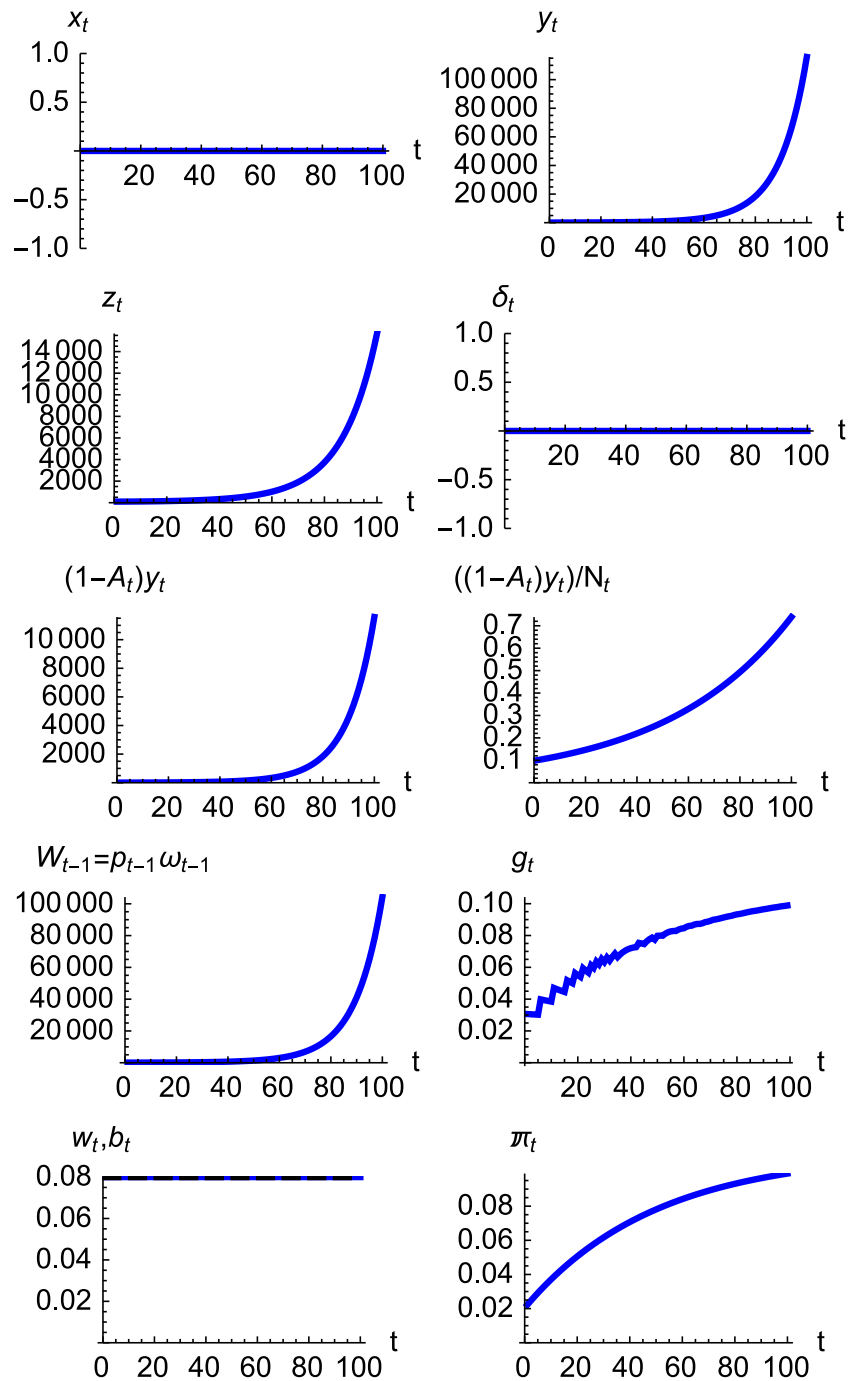
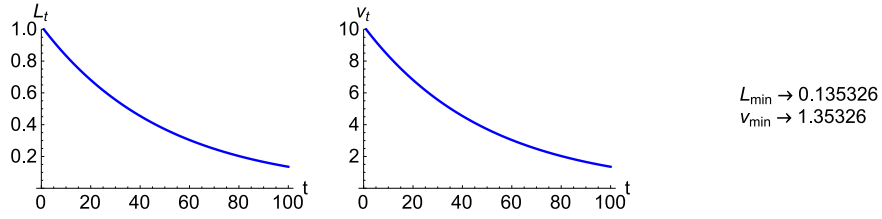


Figure 16: L_t and labour values - Bargaining model with exogenous technical change with $\epsilon = 0$



of wealth in addition to the polarisation of exploitation and class. This polarisation is further reflected in Figure 19(b).

Figure 17: Class and exploitation status - Bargaining model with exogenous technical change with $\epsilon = 0$

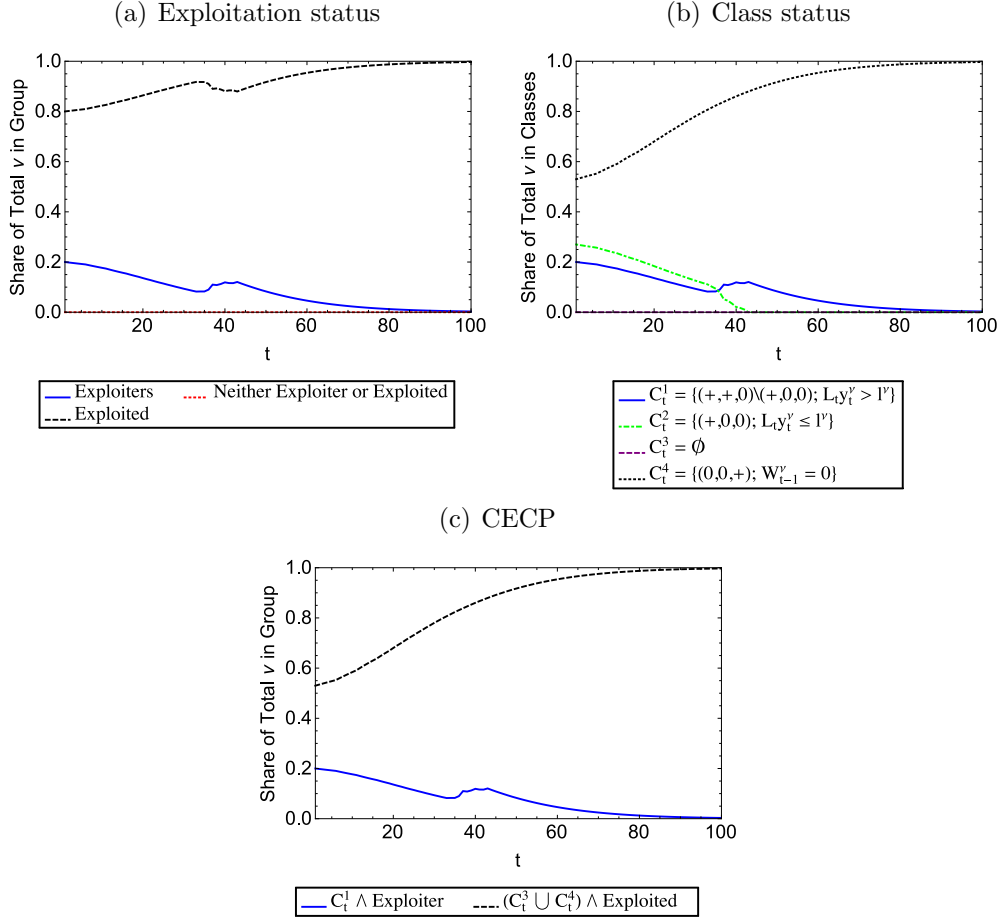
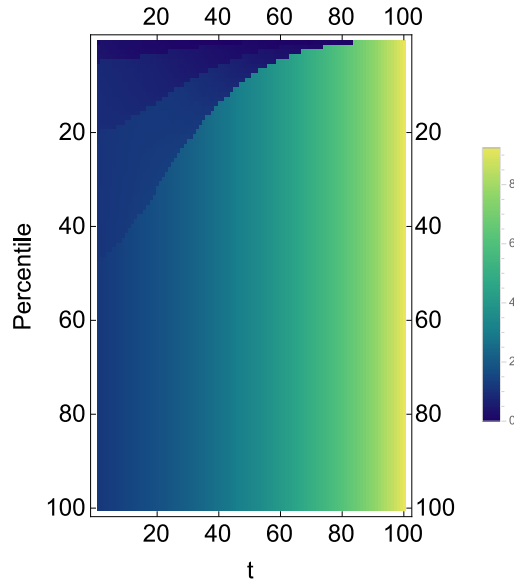
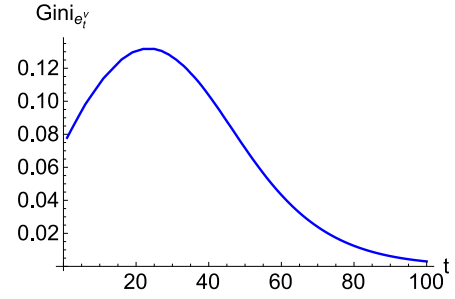


Figure 18: Exploitation intensity index - Bargaining model with exogenous technical change with $\epsilon = 0$

(a) Exploitation intensity index across agents



(b) Gini coefficient of e_t^ν



(c) Distribution of e_t^ν for select t (relative frequency)

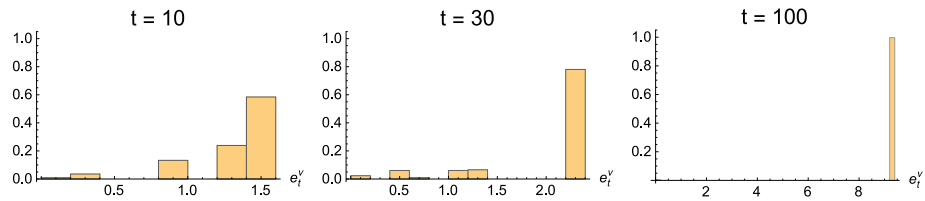
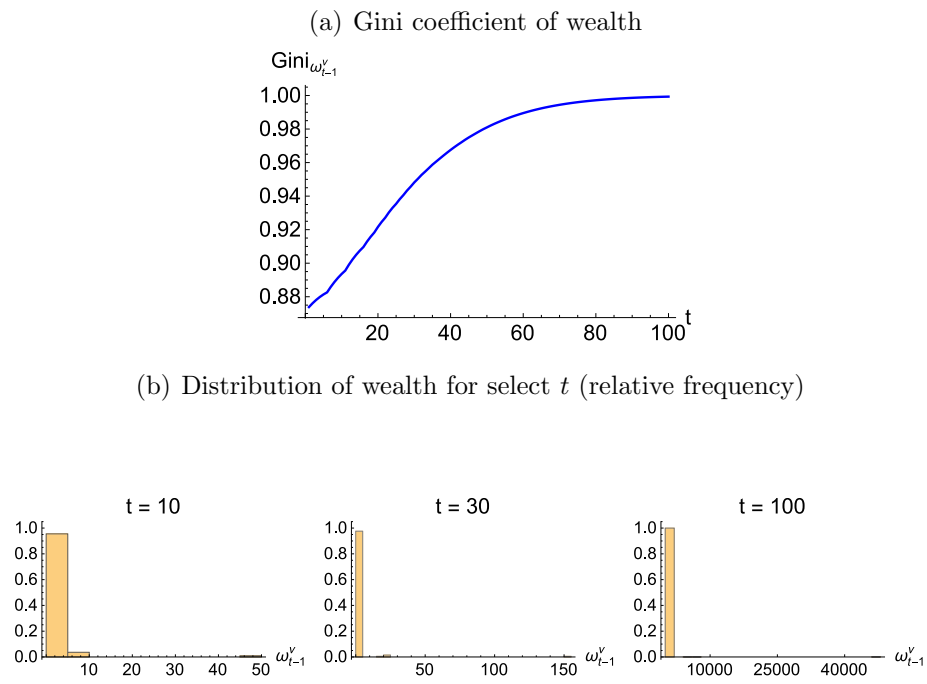


Figure 19: Distribution of wealth - Bargaining model with exogenous technical change with $\epsilon = 0$



3.2 Bargaining model with exogenous technical change and population growth, $\epsilon = 1$

This section examines the bargaining model with exogenous technical change and $\epsilon = 1$. Figure 20 shows the summary results. Because bargaining power lies in the hands of propertyless workers, $\hat{w}_t > b_t$ and $\pi_t = 0$ for all t . Thus, agents are neither exploiters or exploited, $e_t^\nu = 1$ for all ν and all t , and the definitions of class according to Corollary 1 of Theorem 3 do not apply, hence there can be no meaningful correspondence between exploitation and classes. Thus, the diagrams reporting exploitation and classes are omitted. Figures 22(a) and 22(b) show the Gini coefficient of wealth and the distribution of wealth for select t . As expected from $\pi_t = 0$, all agents accumulate from the start of the simulation and new agents arriving with $\omega_{t-1}^\nu = 0$ begin accumulating as well. As a result of universal accumulation the Gini coefficient steadily decreases initially but it starts increasing towards the end of the simulation as the number of agents added to the simulation during each t becomes large, as in section 8.4.2. This result is further reflected in Figure 22(b).

Figure 20: Summary results - Bargaining model with exogenous technical change with $\epsilon = 1$

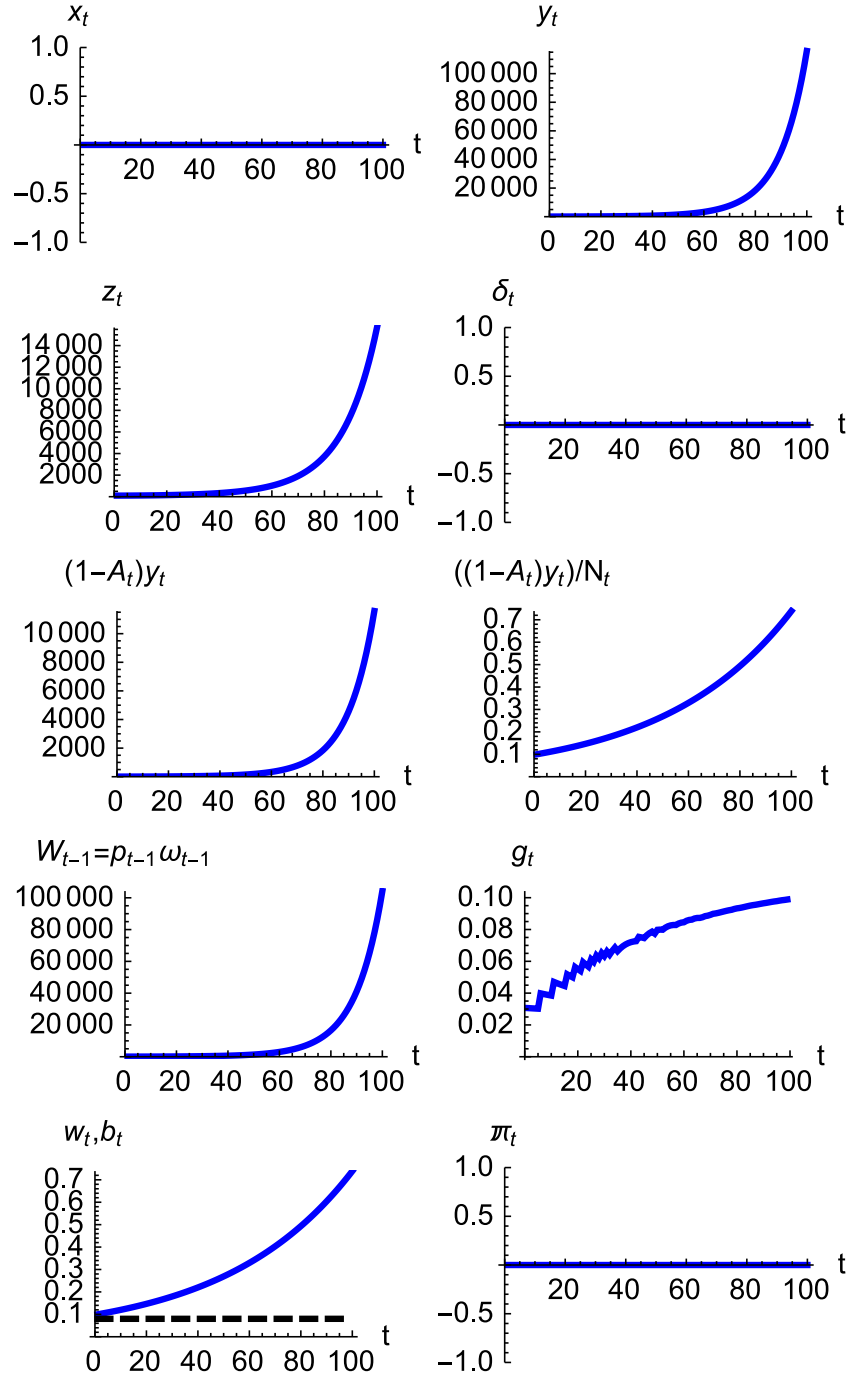


Figure 21: L_t and labour values - Bargaining model with exogenous technical change with $\epsilon = 1$

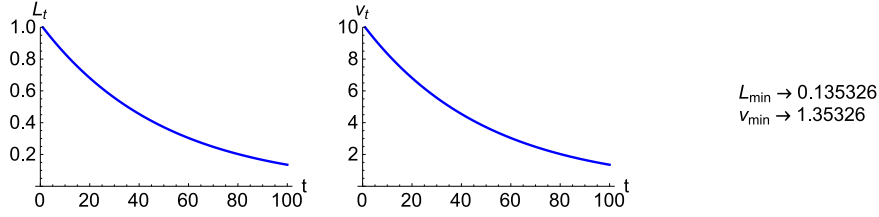
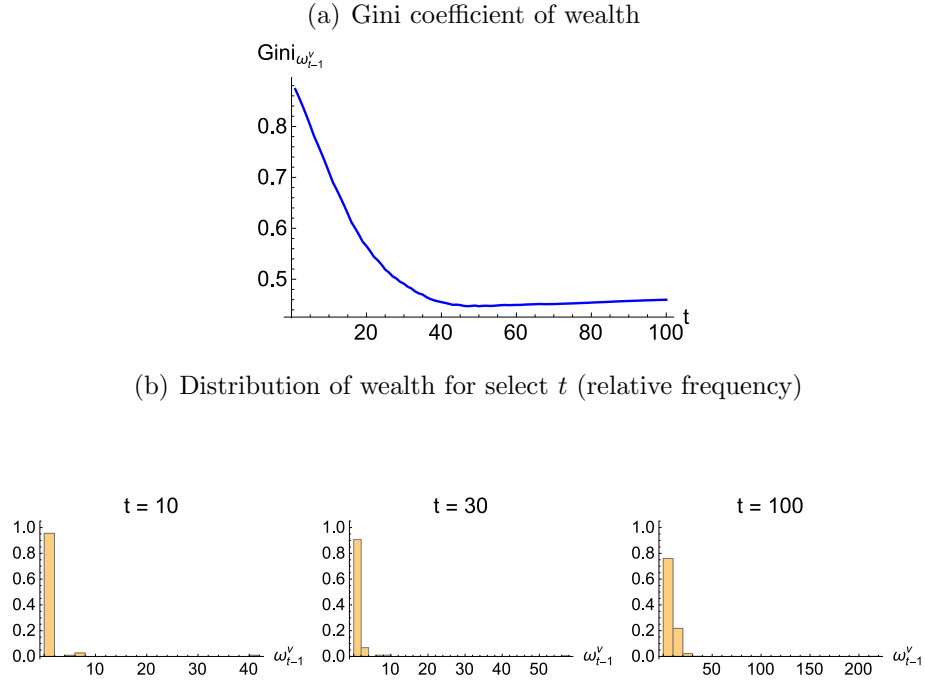


Figure 22: Distribution of wealth - Bargaining model with exogenous technical change with $\epsilon = 1$



3.3 Bargaining model with exogenous technical change and population growth, $\epsilon = 0.0001$

In this section we explore the bargaining model with exogenous technical change and $\epsilon = 0.0001$. The behaviour of the simulation is similar to that in section 8 of the paper for which $\epsilon = 0.002$, but given how the change to the

pattern of technical change affects the rate of population growth (making it lower) smaller values of ϵ allow us to explore the dynamics of the simulation over a longer period of time. Figure 23 shows the summary results of the simulation, which show a growing economy with $\hat{w}_t > b_t$ and $\pi_t > 0$ for part of the simulation until $\pi_t = 0$, as in section 8.4.3.

Figure 25 shows the exploitation and class status of agents. Exploitation exists and there is a correspondence between exploitation status and class until $t = 100$, at which point exploitation and its correspondence to class cease.

A more detailed view of exploitation can be seen in Figures 26(a)-26(c). As Figure 26(a) shows, an increasing percentage of the population experiences greater exploitation intensity up until around $t = 70$, at which point exploitation intensity starts to decrease until $e_t^\nu = 1$ for all ν . This arch-like pattern of exploitation intensity is consistent with the pattern of π_t . Figures 26(b) and 26(c) also reflect the pattern of exploitation: the Gini coefficient of e_t^ν increases for a time and eventually drops to zero and the distribution of e_t^ν for select t shows the dispersion of exploitation until $e_t^\nu = 1$ at the end of the simulation.

Figures 27(a) and 27(b) show the Gini coefficient of wealth and the distribution of wealth for select t . As expected the Gini coefficient of wealth declines over time as agents accumulate even if they begin with $\omega_{t-1}^\nu = 0$. However, towards the end of the simulation there is a reversal in the declining trend of the Gini of wealth as the same population-driven mechanism as in section 8.4.3 of the paper kicks in, as is partially reflected also in Figure 27(b).

Figure 23: Summary results - Bargaining model with exogenous technical change with $\epsilon = 0.0001$

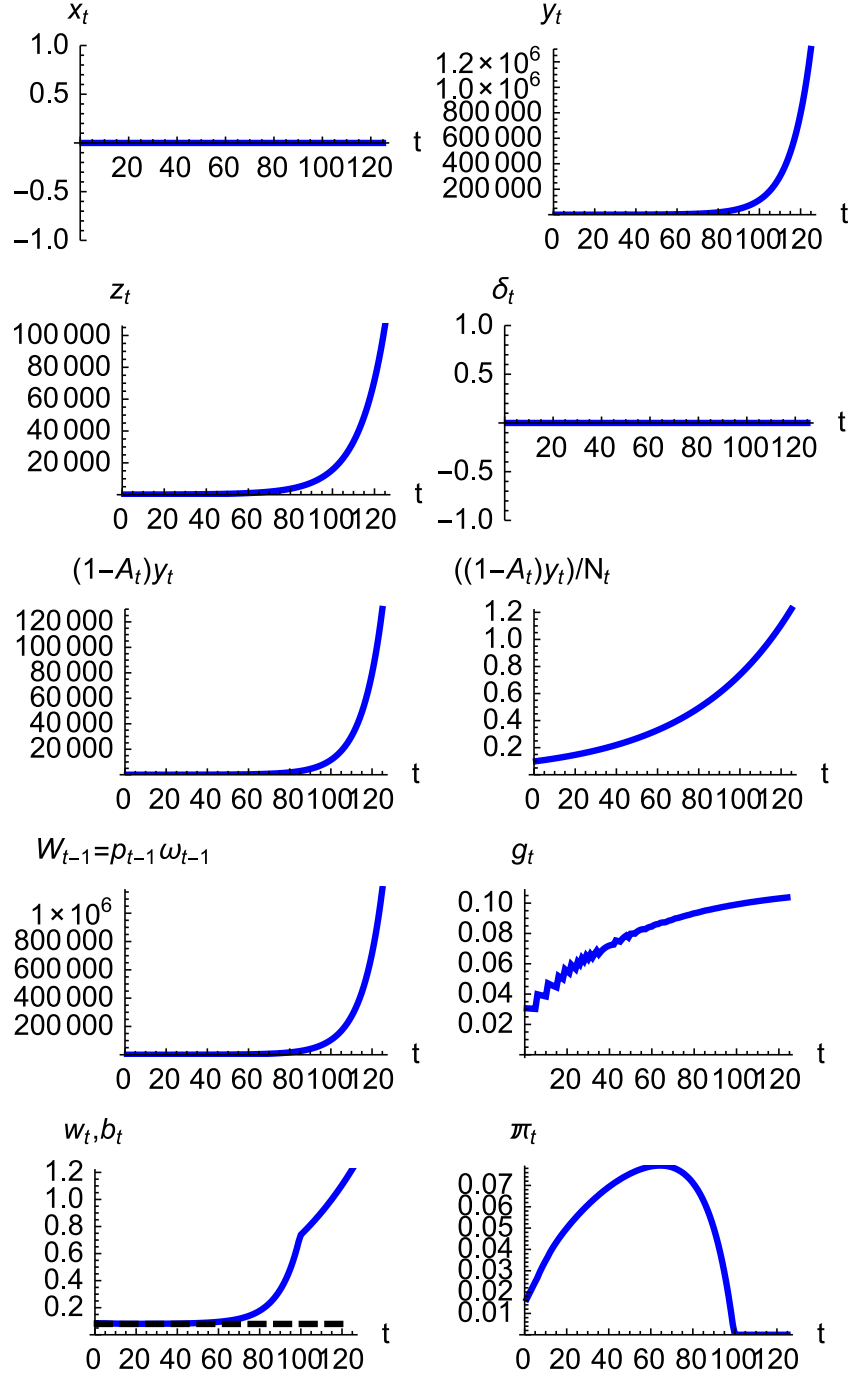


Figure 24: L_t and labour values - Bargaining model with exogenous technical change with $\epsilon = 0.0001$

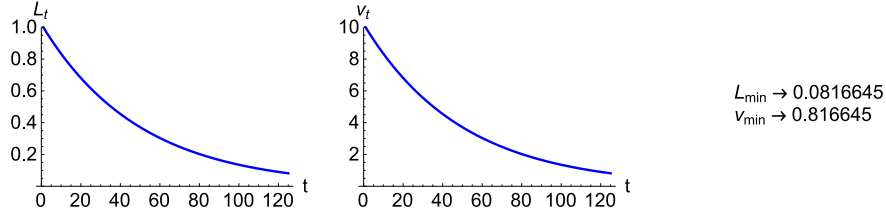


Figure 25: Class and exploitation status - Bargaining model with exogenous technical change with $\epsilon = 0.0001$

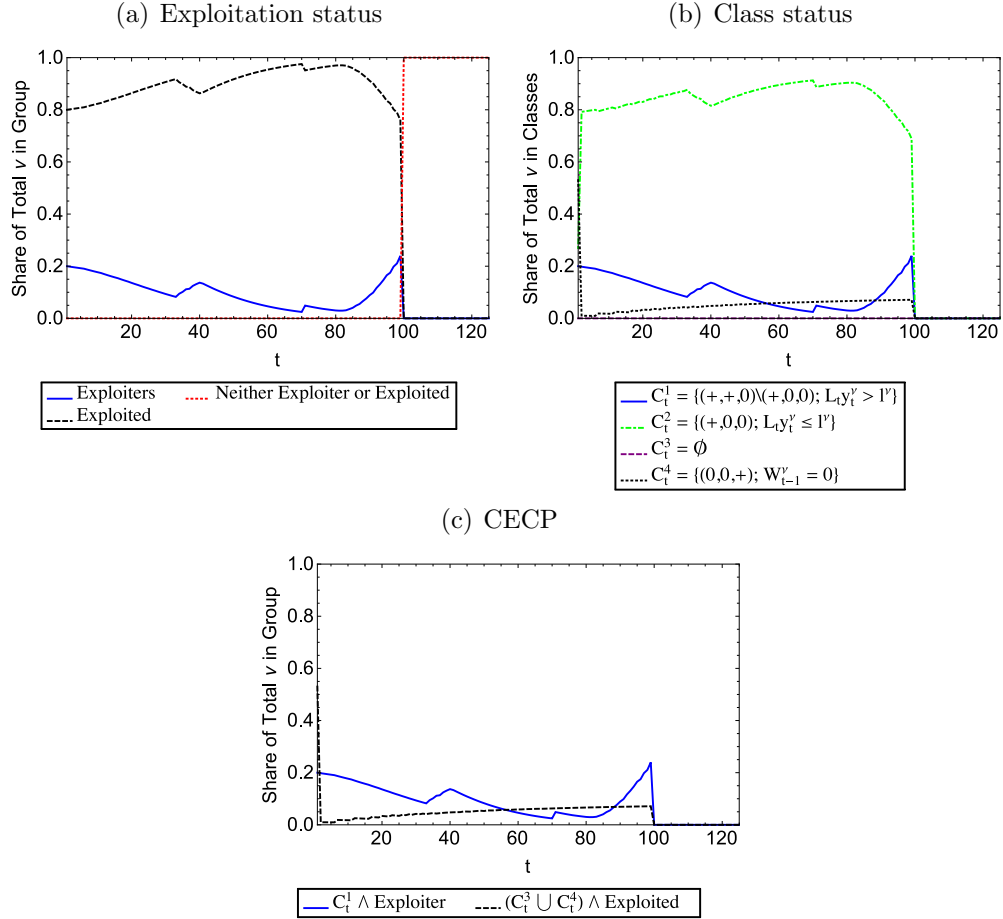
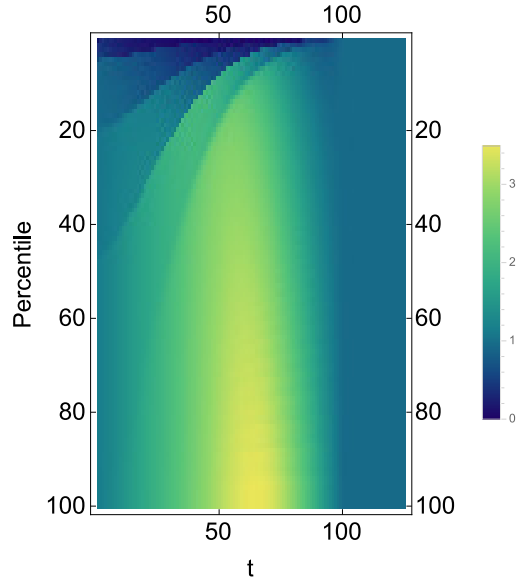
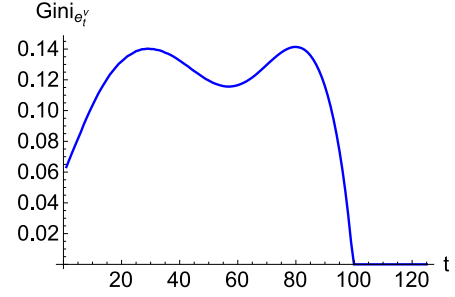


Figure 26: Exploitation intensity index - Bargaining model with exogenous technical change with $\epsilon = 0.0001$

(a) Exploitation intensity index across agents



(b) Gini coefficient of e_t^ν



(c) Distribution of e_t^ν for select t (relative frequency)

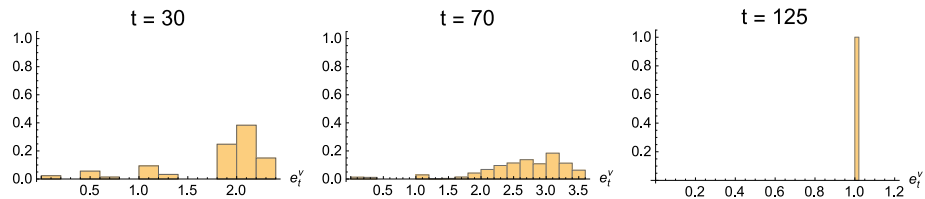
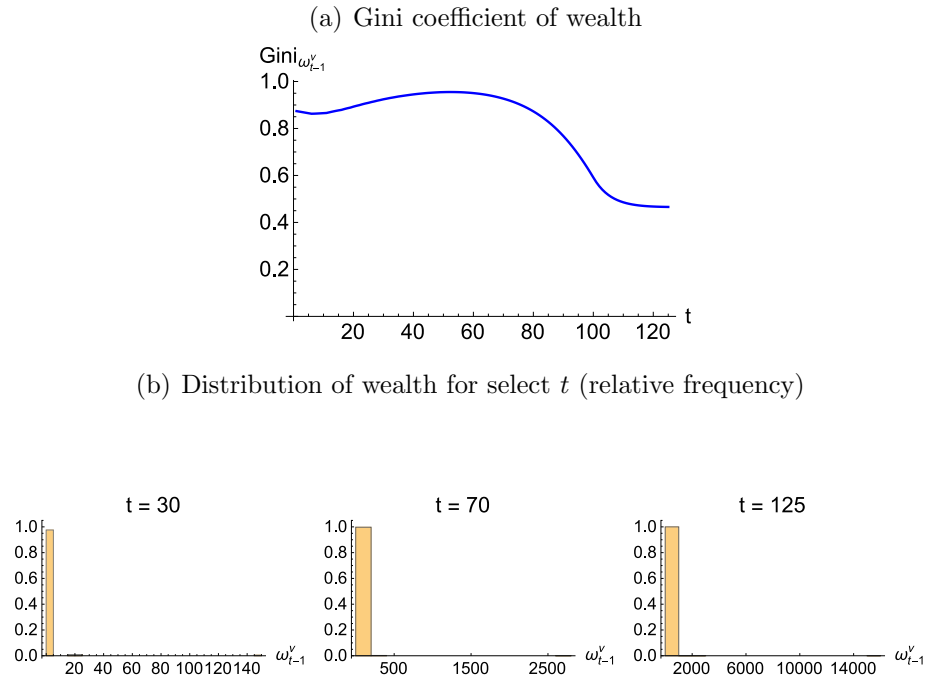


Figure 27: Distribution of wealth - Bargaining model with exogenous technical change with $\epsilon = 0.0001$



4 Alternative wage determinations on the knife-edge

This section explores alternative methods of determining \hat{w}_t on the knife-edge $l = L_t A_t^{-1} \omega_{t-1}$. All initial values and parameters are the same as in sections 6 and 7 of the paper.

4.1 \hat{w}_t determined as midpoint between b_t and $\frac{1}{v_t}$

We modify the basic model to begin on the knife-edge condition $l = L_t A_t^{-1} \omega_{t-1}$ and incorporate technological progress such that this condition is maintained for all t . To be specific, we consider increases in labour productivity such that $1 + \frac{L_{t+1} - L_t}{L_t} = \frac{1}{1+g_t}$, all t .

The consumption norm b_t grows at the same rate as the aggregate endowment, as in previous simulations, and there is a constant N as in the basic model in section 6. The wage \hat{w}_t is determined as the midpoint between b_t and $\frac{1}{v_t}$, where $\hat{w}_t = \frac{1}{v_t}$ implies $\pi_t = 0$.

Figure 28 reports the summary results, which exhibit a similar pattern as those in section 7. The growth rate of aggregate endowments and π_t quickly settle to stable rates, and z_t remains constant at l for all t for reasons discussed in section 7. One slight difference between Figure 28 and previous summary diagrams is that the bottom left panel in Figure 28 reports \hat{w}_t/b_t to show that $\hat{w}_t > b_t$ due to $(\hat{w}_t/b_t) > 1$, albeit only slightly. Figure 29 reports L_t and labour values for all t .

Figure 30 reports the exploitation and class status of agents. Due to $\hat{w}_t > b_t$ and the constancy of $L_t y_t$, the exploitation and class structures remain stable.

Figure 31(a) shows the distribution of the exploitation intensity index e_t^ν over all t , Figure 31(b) shows the gradually decreasing Gini coefficient of e_t^ν , and Figure 31(c) shows the distribution of e_t^ν for select t . Figures 32(a) and 32(b) show the Gini coefficient of wealth and the distribution of ω_{t-1} for select t . As expected, because $\hat{w}_t > b_t$, the Gini of wealth gradually decreases as all agents accumulate, and poorer agents accumulate faster than wealthier ones.

Figure 28: Summary results - Model with \hat{w}_t as midpoint between b_t and $\frac{1}{v_t}$

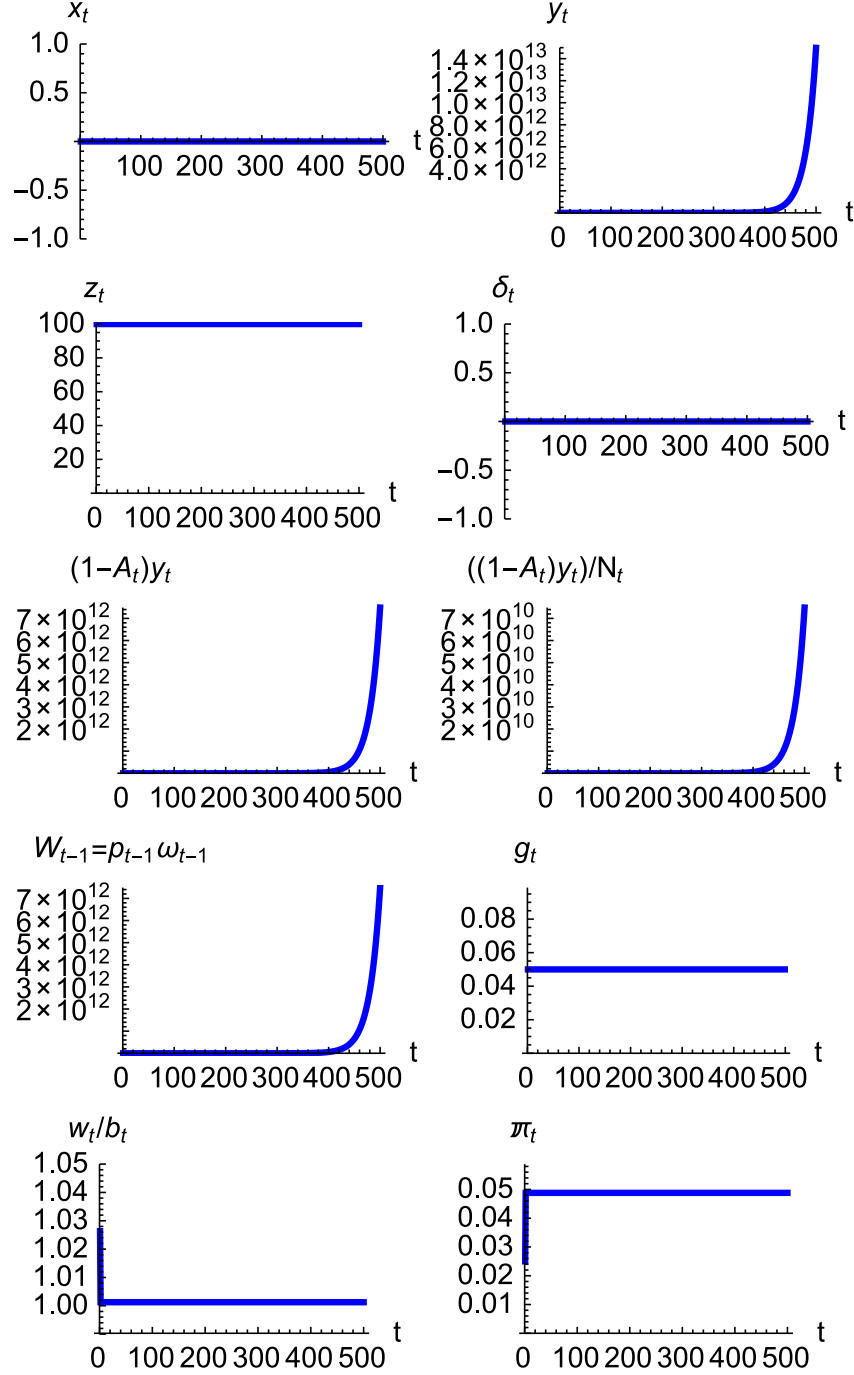


Figure 29: L_t and labour values - Model with \hat{w}_t as midpoint between b_t and $\frac{1}{v_t}$

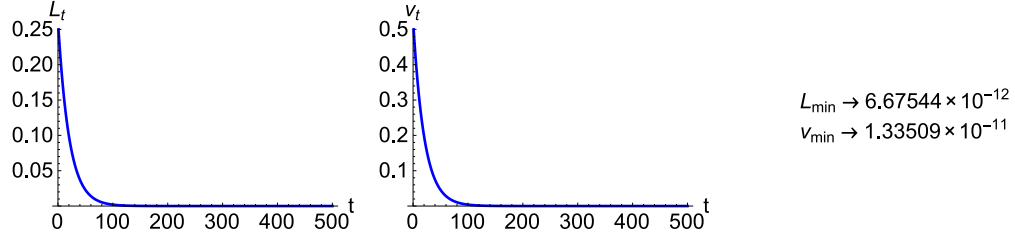


Figure 30: Class and exploitation status - Model with \hat{w}_t as midpoint between b_t and $\frac{1}{v_t}$

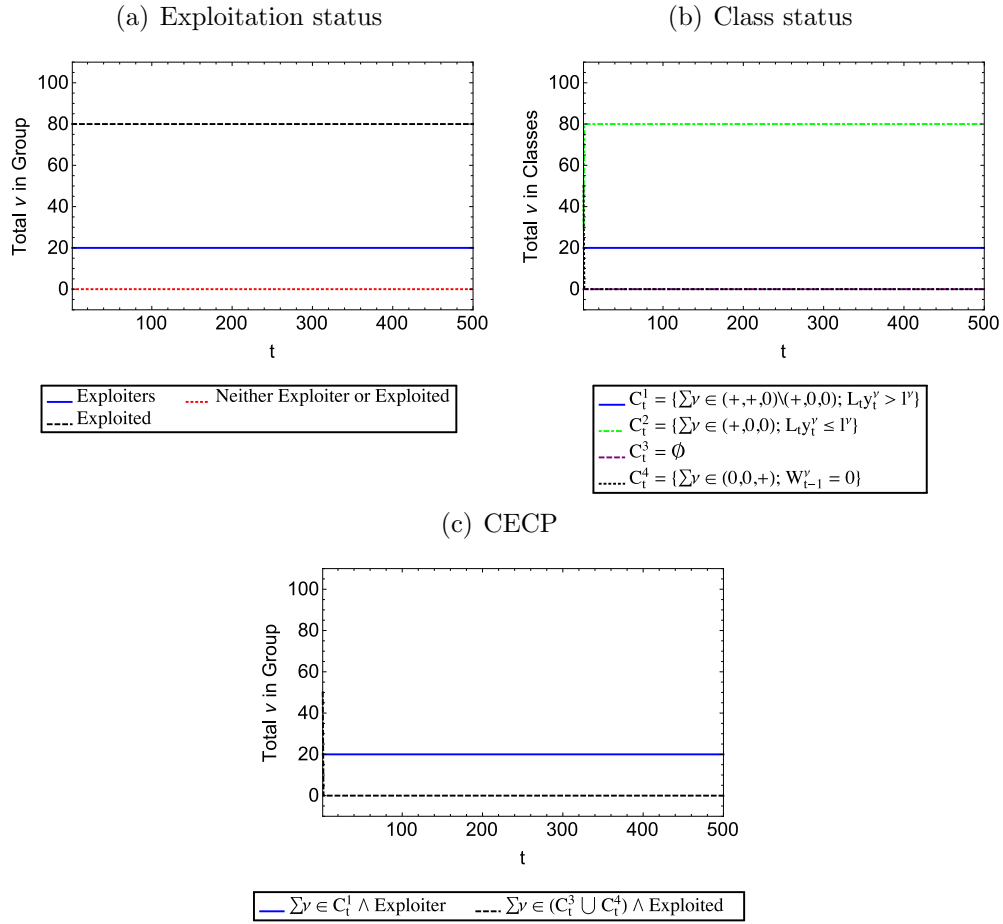


Figure 31: Exploitation intensity index - Model with \hat{w}_t as midpoint between b_t and $\frac{1}{v_t}$

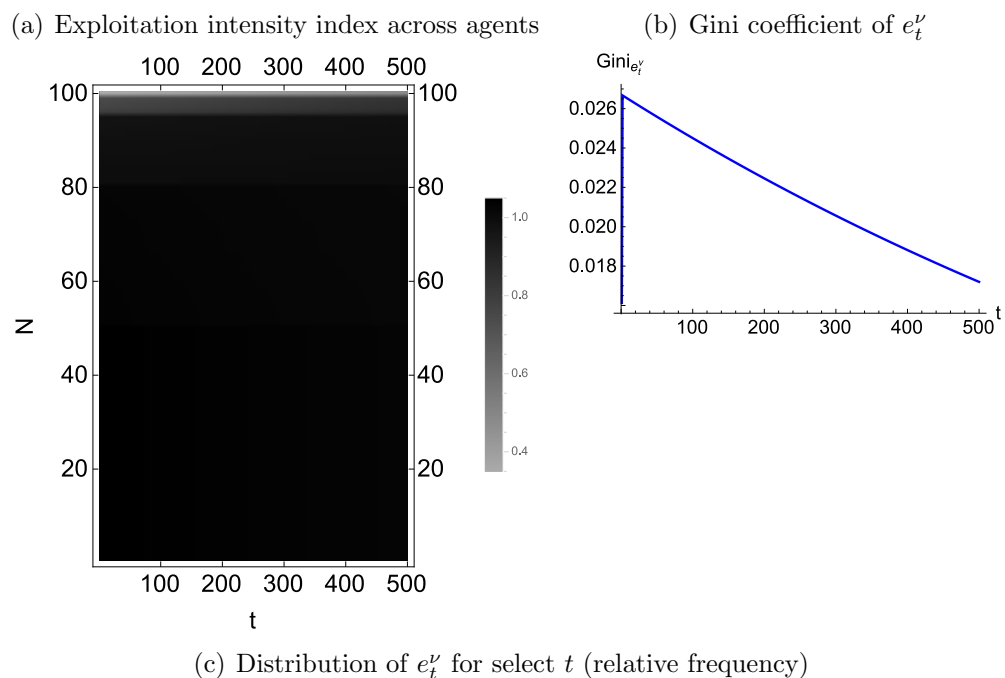
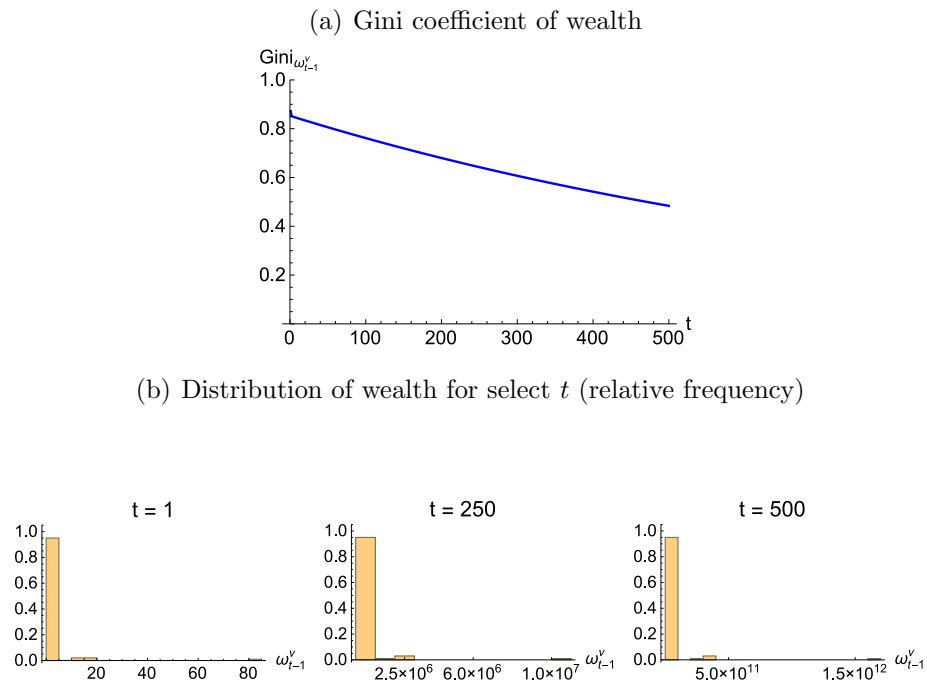


Figure 32: Distribution of wealth - Model with \hat{w}_t as midpoint between b_t and $\frac{1}{v_t}$



4.2 \hat{w}_t determined randomly between b_t and $\frac{1}{v_t}$

Next, we modify the model in the previous section to assume that the wage \hat{w}_t during each t is randomly selected in the inclusive range of b_t to $\frac{1}{v_t}$.

Figure 33 reports the summary results, which are similar to those of the previous section and section 7 of the paper, except for the movement in \hat{w}_t/b_t and π_t shown in the bottom panels, which is a reflection of the random determination of \hat{w}_t . Figure 34 reports L_t and labour values.

Figure 35 reports the exploitation and class status of agents. As in the previous section, due to $\hat{w}_t > b_t$ and the constancy of $L_t y_t$, the exploitation and class structures remain stable over the simulation.

Figure 36(a) shows the distribution of the exploitation intensity index e_t^ν for all t , Figure 36(b) shows the gradually decreasing Gini coefficient of e_t^ν , and Figure 36(c) shows the distribution of e_t^ν for select t . Figures 37(a) and 37(b) show the Gini coefficient of wealth and the distribution of ω_{t-1} for select t . As expected, because $\hat{w}_t > b_t$, the Gini of wealth decreases as all agents accumulate, and poorer agents accumulate faster than wealthier ones.

Figure 33: Summary results - Model with \hat{w}_t randomly between b_t and $\frac{1}{v_t}$

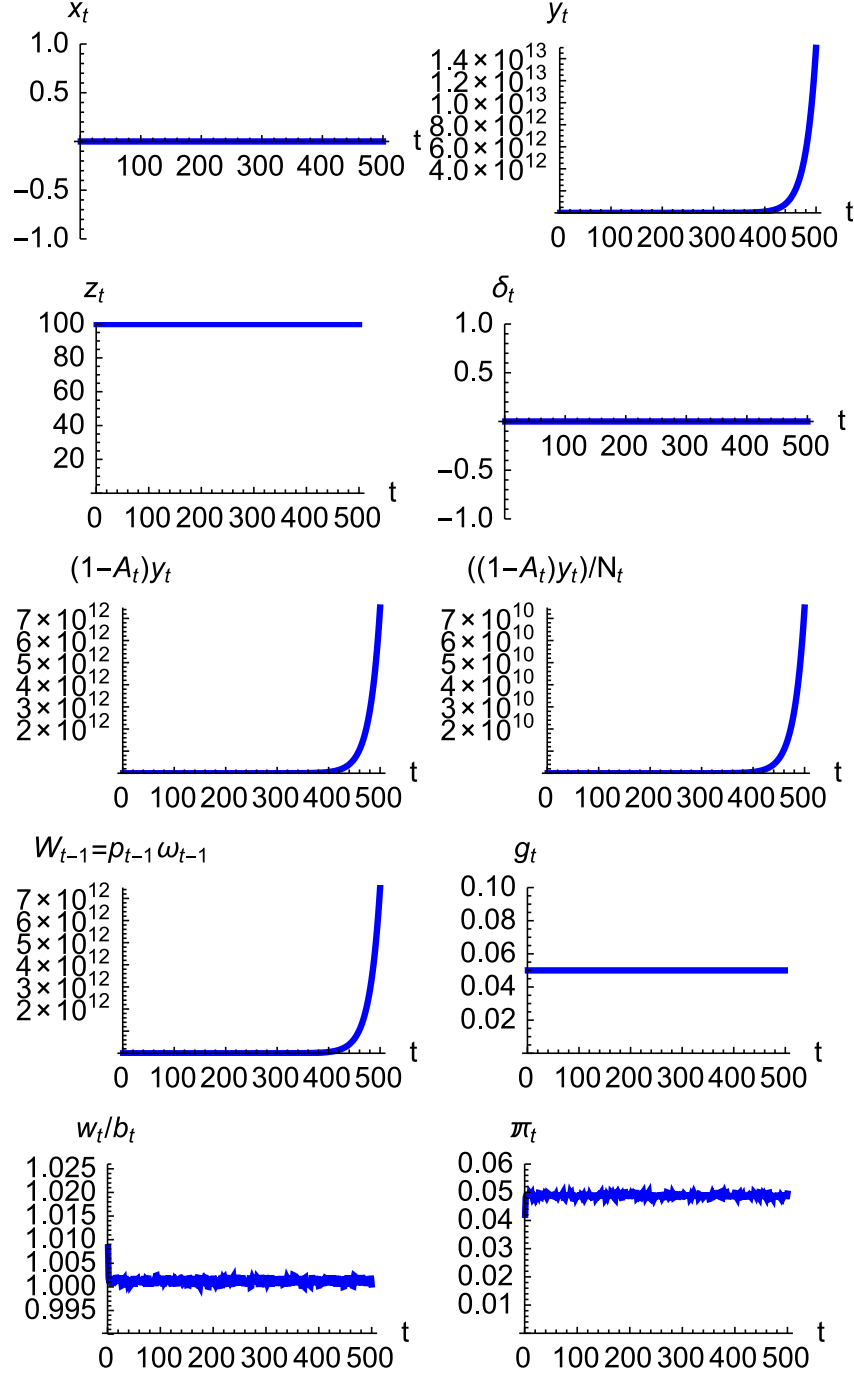


Figure 34: L_t and labour values - Model with \hat{w}_t randomly between b_t and $\frac{1}{v_t}$

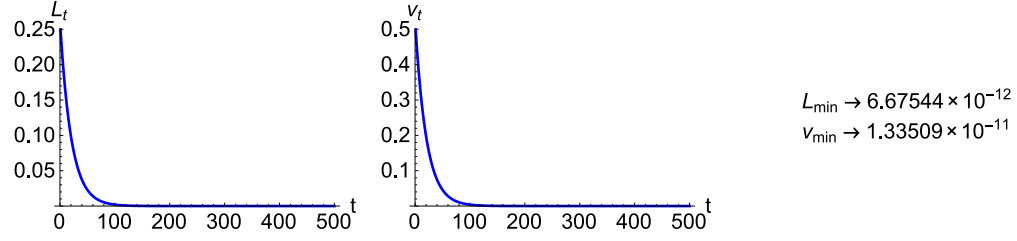


Figure 35: Class and exploitation status - Model with \hat{w}_t randomly between b_t and $\frac{1}{v_t}$

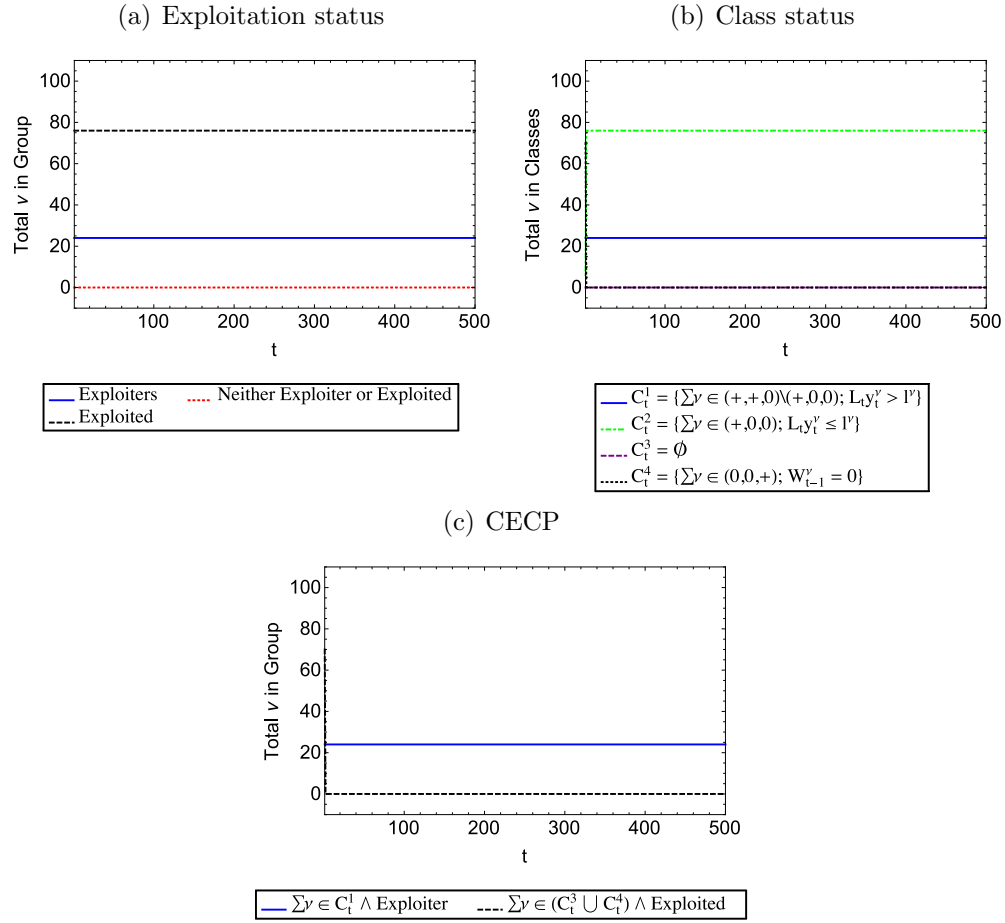


Figure 36: Exploitation intensity index - Model with \hat{w}_t randomly between b_t and $\frac{1}{v_t}$

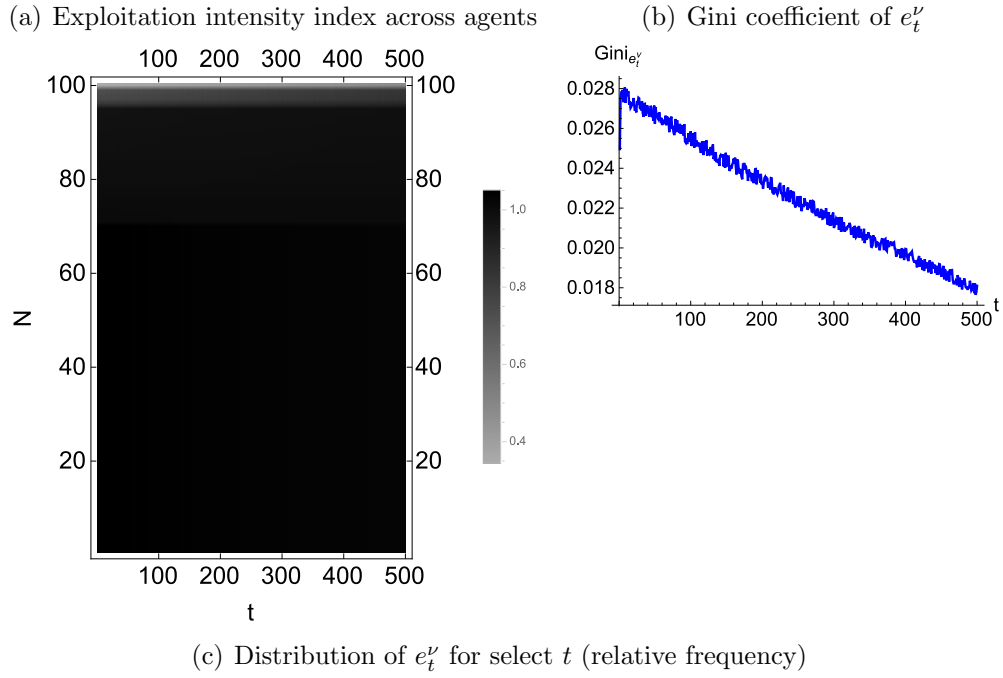
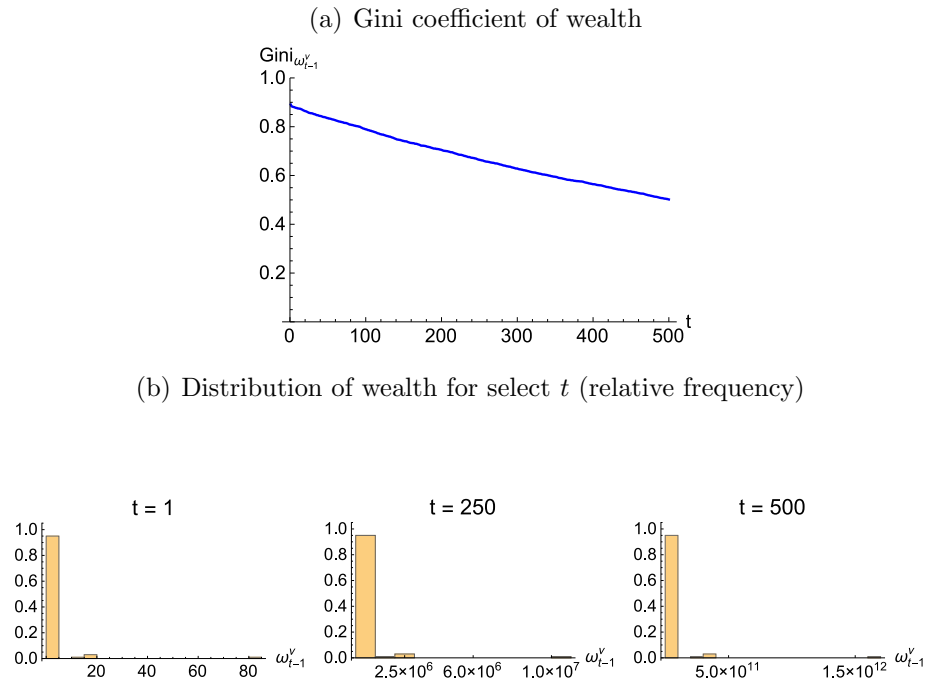


Figure 37: Distribution of wealth - Model with \hat{w}_t randomly between b_t and $\frac{1}{v_t}$



4.3 \hat{w}_t as an increasing function of g_t

Finally, we modify the model in the previous sections to assume that the wage \hat{w}_t during each t is determined as an increasing function of the accumulation rate g_t , according to the following formula:

$$\hat{w}_t = k_t \frac{1}{v_t} + (1 - k_t)b_t,$$

where $k_t = 1 - \frac{1}{1+g_t}$. At the beginning of the simulation $\hat{w}_0 = b_0$ but $\hat{w}_t > b_t$ for all $t > 0$.

Figure 38 reports the summary results. As in section 7 of the paper, g_t and π_t remain stable and constant over the course of the simulation, however unlike in section 7, $\hat{w}_t > b_t$ for all t . Figure 39 reports L_t and labour values.

Figure 40 reports the exploitation and class status of agents. As in the preceding sections, and for the same reasons, the exploitation and class structures remain stable over the simulation.

Figure 41(a) shows the distribution of the exploitation intensity index e_t^ν for all t , Figure 41(b) shows the gradually decreasing Gini coefficient of e_t^ν , and Figure 41(c) shows the distribution of e_t^ν for select t . Figures 42(a) and 42(b) show the Gini coefficient of wealth and the distribution of ω_{t-1} for select t . As expected, because $\hat{w}_t > b_t$, the Gini of wealth decreases as all agents accumulate, and poorer agents accumulate faster than wealthier ones.

Figure 38: Summary results - Model with \hat{w}_t as an increasing function of g_t

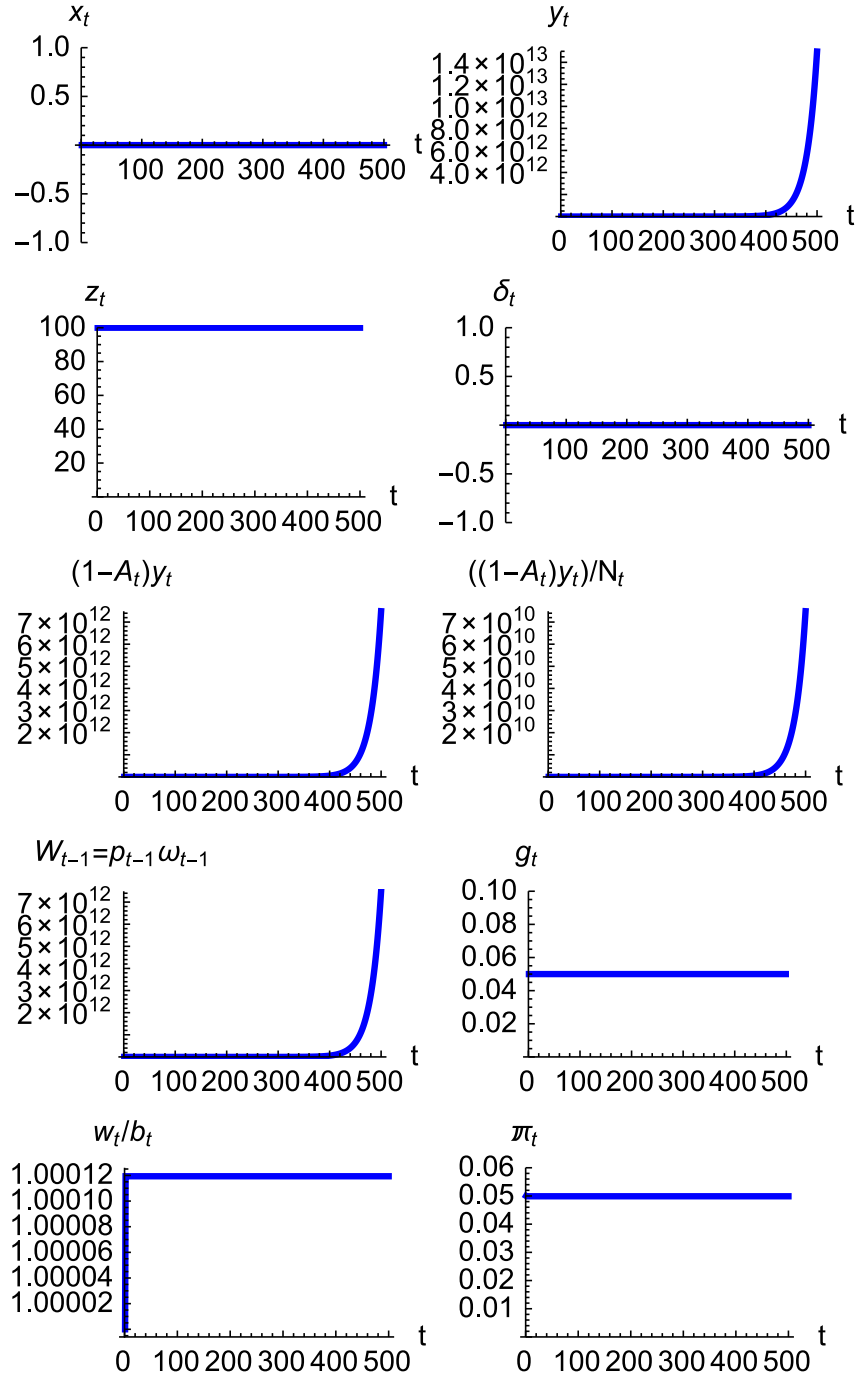


Figure 39: L_t and labour values - Model with \hat{w}_t as an increasing function of g_t

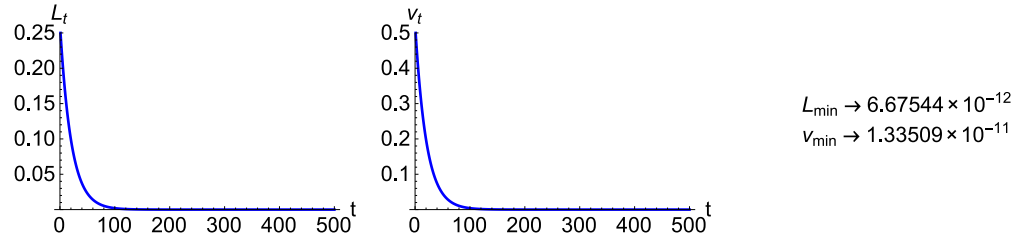


Figure 40: Class and exploitation status - Model with \hat{w}_t as an increasing function of g_t

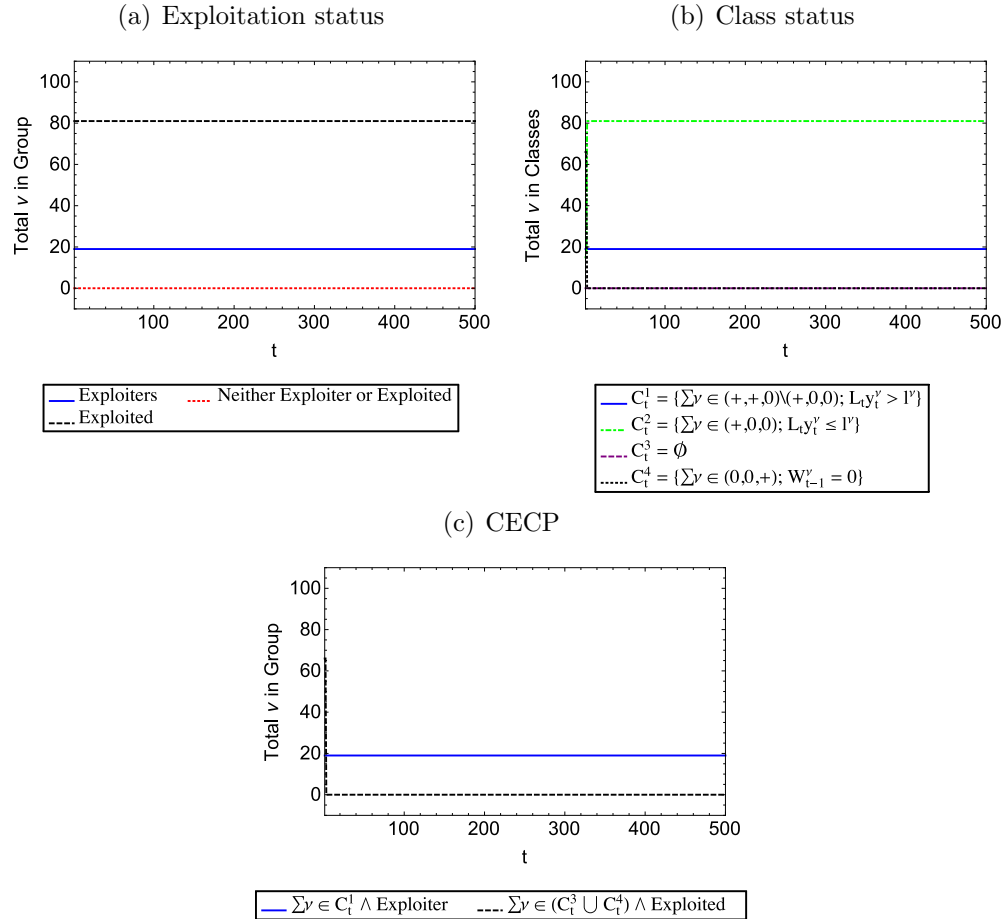


Figure 41: Exploitation intensity index - Model with \hat{w}_t as an increasing function of g_t

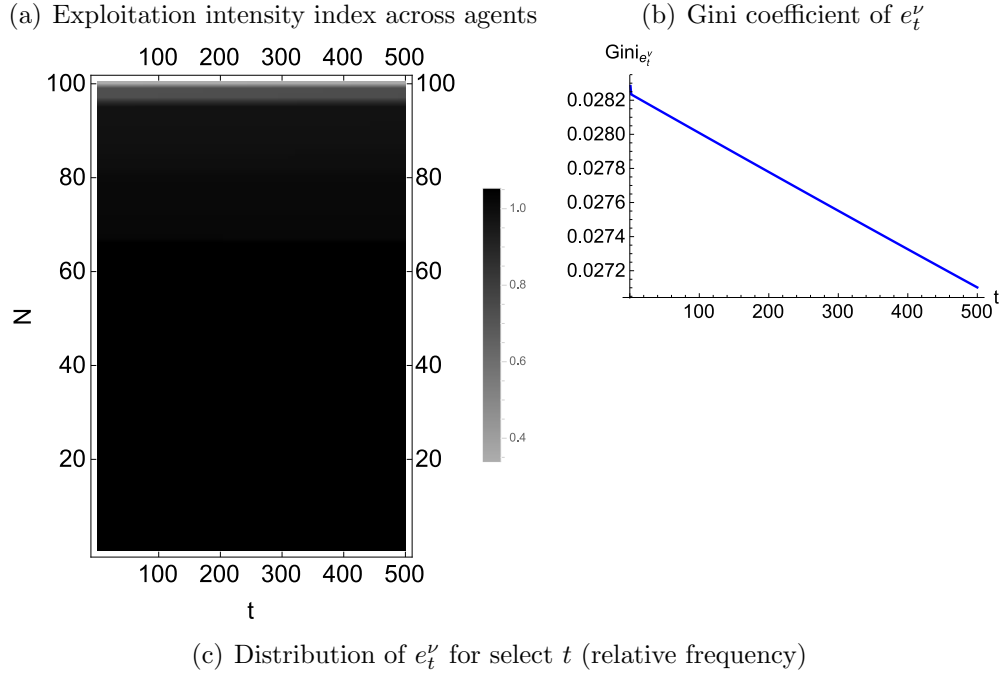
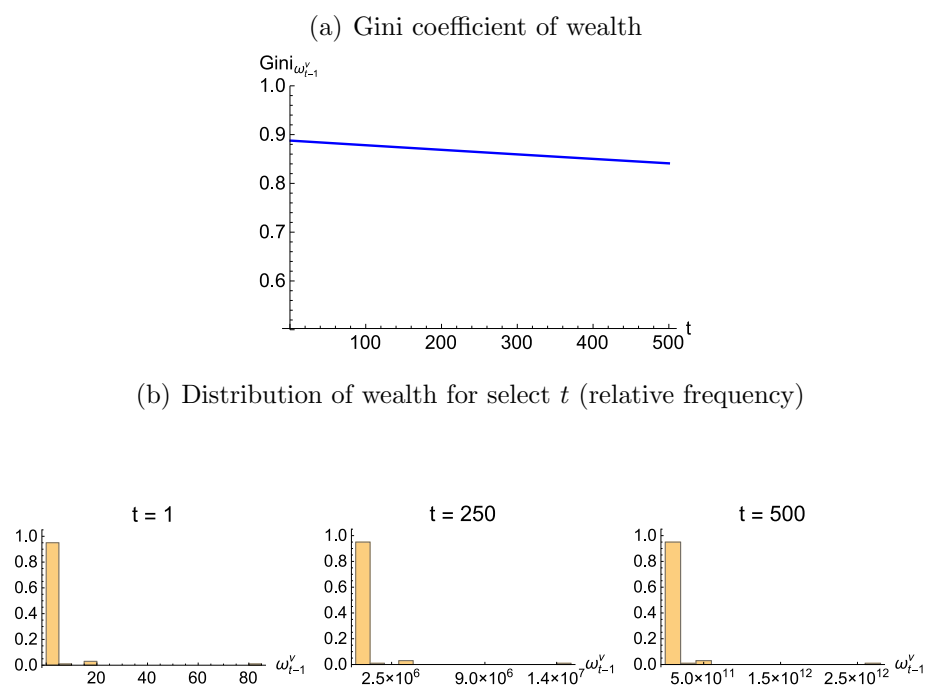


Figure 42: Distribution of wealth - Model with \hat{w}_t as an increasing function of g_t



5 An alternative representation of class

In the paper, we follow Roemer [1] and define the main classes as follows:

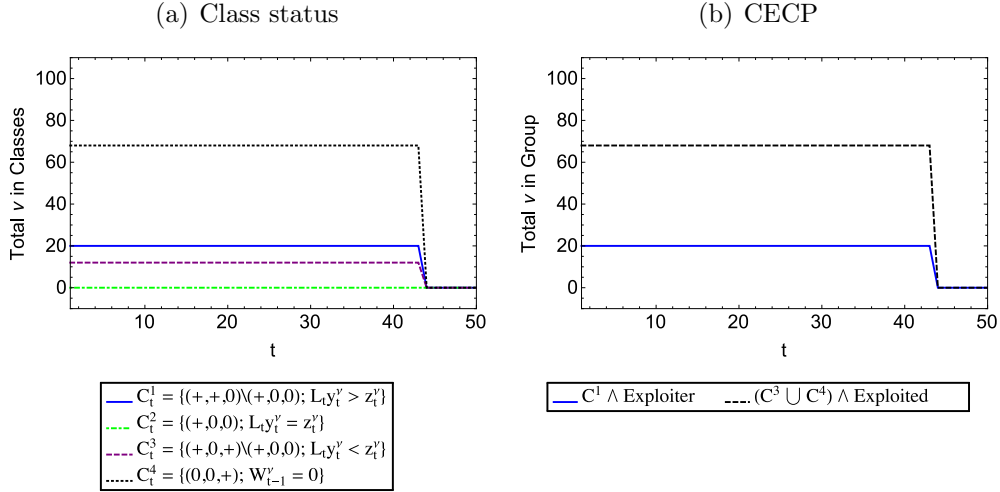
$$\begin{aligned} C_t^1 &= \{\nu \in \mathcal{N} \mid \mathcal{A}^\nu(1, w_t) \text{ has a solution of the form } (+, +, 0) \setminus (+, 0, 0)\}, \\ C_t^2 &= \{\nu \in \mathcal{N} \mid \mathcal{A}^\nu(1, w_t) \text{ has a solution of the form } (+, 0, 0)\}, \\ C_t^3 &= \{\nu \in \mathcal{N} \mid \mathcal{A}^\nu(1, w_t) \text{ has a solution of the form } (+, 0, +) \setminus (+, 0, 0)\}, \\ C_t^4 &= \{\nu \in \mathcal{N} \mid \mathcal{A}^\nu(1, w_t) \text{ has a solution of the form } (0, 0, +)\}. \end{aligned}$$

In Corollary 1, we prove that at all equilibria with $\pi_t > 0$, the class status of an agent is determined by the difference between labour demand and *potential* labour supply, which coincides with the agent's labour endowment.

Yet, one may argue that classes should be defined based on agents' actual choices, and in particular on their choices within labour relations. Therefore in this section we analyse the class structure and the relation between class and exploitation status in all of our models based on agent's actual choices. The results are remarkably similar to those obtained in the paper.

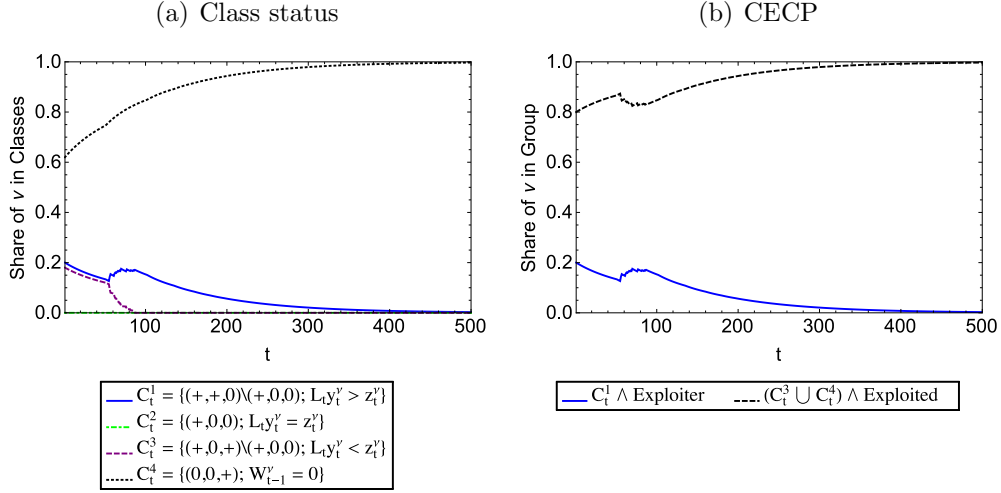
For the basic model:

Figure 43: Class status (alternative definition) - Basic model



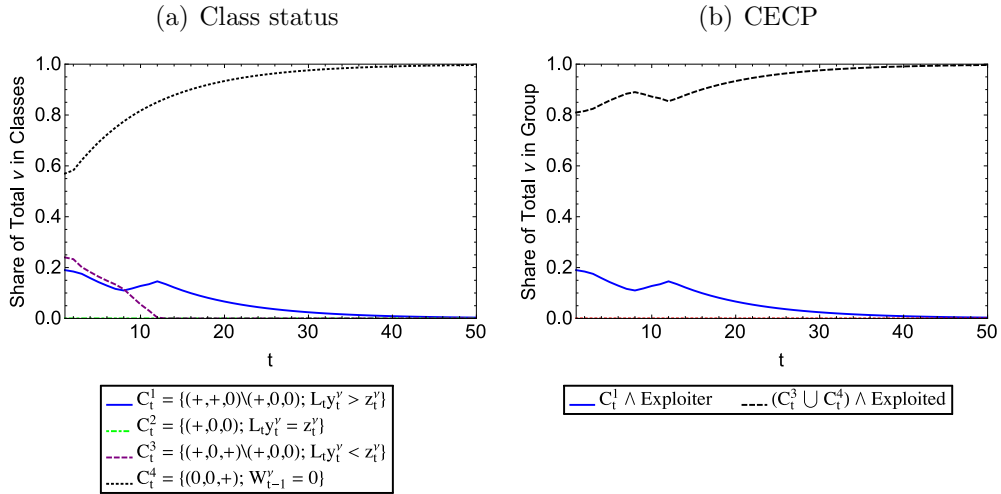
For the model with endogenous subsistence and technical change:

Figure 44: Class status (alternative definition) - Model with exogenous technical change and population growth



For the model with wage bargaining and $\epsilon = 0$:

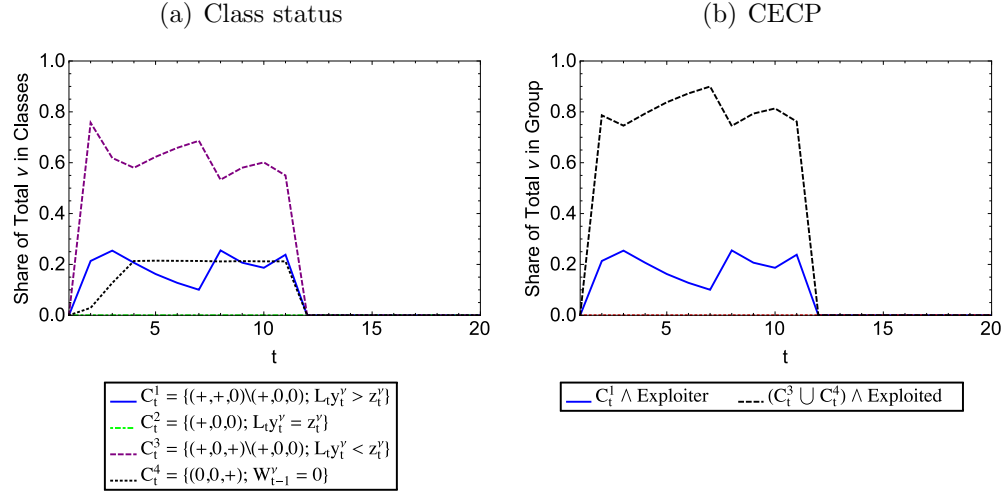
Figure 45: Class status (alternative definition) - Bargaining model with $\epsilon = 0$



The results for the model with wage bargaining and $\epsilon = 1$ are omitted, as in the paper, since $\pi_t^{N(\sigma_t)} = 0$ and the defined set of classes does not hold.

For the model with wage bargaining and $\epsilon = 0.002$:

Figure 46: Class status (alternative definition) - Bargaining model with $\epsilon = 0.002$



References

- [1] Roemer, J.E., 1982. *A General Theory of Exploitation and Class*. Harvard University Press, Cambridge, MA.